Università degli Studi di Ferrara

DOTTORATO DI RICERCA
IN
FARMACOLOGIA E ONCOLOGIA MOLECOLARE

CICLO XXVIII

COORDINATORE Chiar.mo Prof. Antonio Cuneo

Accelerated Tumor Progression in Mice Lacking the ATP Receptor P2X7

Settore Scientifico Disciplinare: Patologia clinica MED/05

Dottorando
Dott.ssa Marina Capece

Tutore
Chiar.mo Prof. Francesco Di Virgilio

Co-tutore
Dott.ssa Elena Adinolfi

Anni 2013/2015

INDEX

INTRODUCTION

Adenosine Triphosphate

Adenosine triphosphate (ATP) is a nucleoside triphosphate used by cells as the molecular unit of currency of intracellular energy transfer [1]. ATP was discovered in 1929 by Karl Lohmann [2], and independently by Cyrus Fiske and Yellapragada Subbarow of Harvard Medical School [3].

The structure of this molecule consists of a purine base (adenine) attached by the 9' nitrogen atom to the 1' carbon atom of a pentose sugar (ribose). Three phosphate groups are attached at the 5' carbon atom of the pentose sugar. It is the addition and removal of these phosphate groups that inter-convert ATP, ADP and AMP, and the two phosphoanhydride bonds are responsible for the high energy content of this molecule.

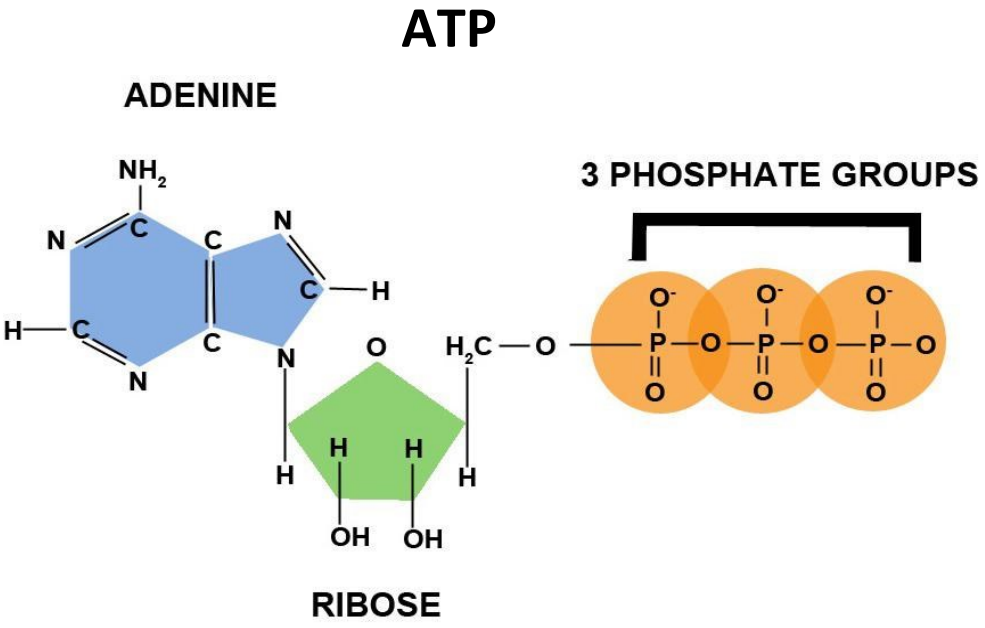

Figure 1. Structure of ATP**.** ATP consists of adenosine, composed of an adenine ring and a ribose sugar, and three phosphate groups (triphosphate).

ATP is a key nucleotide involved in several important cell mechanisms. The intracellular role as energy source for the cells has been recognized for many years: cells have mechanisms for synthesizing, maintaining or rapidly restoring the intracellular level of ATP. In mammalian the ATP concentration in the intracellular compartment is 5-10 mM, but can reach much higher levels in specific intracellular stores, where the nucleotide

concentration reach 100 mM. On the contrary, the extracellular ATP concentration in physiological conditions, is much lower and it is in the nanomolar range (20-50 nM) [4].

ATP as extracellular messenger

The huge intra/extracellular concentration ATP gradient on the one hand accelerates enormously the speed of release of this nucleotide in response to the opening of plasma membrane ATP-conducing pathways, and on the other increases the signal-to-noise ratio, the background noise being almost null [5]. Furthermore, ATP is highly water soluble, and thus easily diffusible in the aqueous extracellular environment, and quickly degraded by a series of powerful nucleotidases [6]. Moreover, virtually all eukaryotic cells are able to release ATP and are equipped with specific receptors for it (see below) [7]. Thus, ATP has all the characteristics of an ideal second messenger, and the biological rationale of the release of this nucleotide in extracellular microenvironment is exactly its role as an extracellular messenger. This ATP property was demonstrated for the first time in 1929 by Drury and Szent-Györgyi, who observed that extracellular ATP induces decrease of the strength and the velocity of cardiac muscle contraction. Moreover thirty years later was found that during antidromic stimulation of sensory nerves of the ear artery, the ATP was released in sufficient concentration to affect the muscular tone [8]. Anyway the effective breakthrough came in 1972 when Geoffrey Burnstock demonstrated that ATP act as neurotransmitter, released by purinergic terminations in central nervous system neurons or in smooth muscle cells, and binds membrane receptors [9]. In addition, Burnstock proposed the existence of two families of purinergic receptors, P1 and P2, capable to mediate effects of respectively adenosine and ATP, that will be discussed later in this work [10, 11].

ATP in inflammation and cancer

A homeostatic system should be able to release an array of intracellular messengers capable of signaling cell and tissue damage. The simplest way to signal cell distress is to develop a receptor system that senses in the extracellular space the presence of molecules that are normally sequestered intracellularly. Therefore, it is not a surprise that the most powerful and ubiquitous signal of distress or damage (otherwise known as DAMP, damage-associated molecular pattern) is ATP. Of course, ATP is not the only DAMP used by multicellular organisms to signal danger, but it is likely to be the most ancient [5].

High concentrations of extracellular ATP are associated to inflammatory conditions, since the nucleotide is released by injured cells and by activated immune system cells [12, 13] [14, 15]. In fact, ATP may be released by dying cells in response to non-programmed cues, such as the necrosis produced by pressure disruption, hypoxic injury, toxins, infection and trauma [16].

In our laboratory it was also developed a bioluminescence probe, called pmeLUC, for the measurement of extracellular ATP both *in vitro* and *in vivo.* This probe is a plasma membrane luciferase, with the ATP catalytic site facing the extracellular side, which can be transfected in reporter cells that are subsequently inoculated into the tumor mass [17]. Thanks to this molecular device it was demonstrated that even the extracellular microenviroment of tumors contains relatively high concentration of ATP, in hundreds of micromolar range [18]. ATP was thought to be secreted by cancer cells [18, 19], but it has been postulated that the main source for ATP could be depend on dying cells [20], such as those in the perilesional hypoxic regions of solid tumors [21]. Once accumulated in the tumor microenvironment, ATP exerts effect that are beneficial or detrimental to the host depending on: (i) its concentration, (ii) the ATP receptor subtypes involved and (iii) the expression levels of nucleotide-degrading enzymes in immune, cancerous and stromal cells, composing the complex tumor milieu [22]. Here, ATP acts as a trophic factor, danger signal and main source of the immunosuppressant adenosine, emerging as a new and potent regulator of cancer growth progression and immune response modulation.

Purinergic receptor

It was early anticipated in this work that were discovered and classified two families of purinergic receptors, P1 and P2, capable to mediate effects of respectively adenosine and nucleotide. Extracellular ATP is the natural ligand of P2Y metabotropic and P2X inotropic receptors, both belonging to the P2 subfamily [10, 23]. Table 1 shows the complete purinergic receptors classification.

Receptor	Ligands[5,7]	Ligand binding affinities EC_{50} (μM)[7]	Desensitization rate or G-protein coupling[16,45]	Main downstream signalling events[16]	Expression in different immune cell types[7]						
					Neutrophils[12]	Monocytes	Macrophages	Dendritic cells	T cells	B cells[85]	NK cells[86]
P2X ATP receptors											
P2X1	ATP	0.05–1	<1 s	Ca^{2+} and Na^{+} influx	+	+	+	+	+	+	+
P2X2	ATP	1–30	>20 s	Ca^{2+} influx	ND	ND	ND	ND	ND	+	ND
P2X3	ATP	0.3–1	<1 s	Cation influx	ND	ND	ND	ND	ND	+	+
P2X4	ATP	1–10	>20 s	Ca^{2+} influx	+	+	+	+	+	+	+
P2X5	ATP	1–10	>20 s	Ion influx	+	+	+	+	+	+	ND
P2X6	ATP	1–12	-	Ion influx	ND	ND	ND	ND	ND	+	+
P2X7	ATP	>100	>20 s	Cation influx and pore formation	+	+	+	+	+	+	+
*P2Y nucleotide receptors**											
P2Y1	ADP	8	$G_{q/11}$	PLCβ activation	+	+	+	+	+	+	+
P2Y2	ATP, UTP	0.1 (ATP), 0.2 (UTP)	$G_{q/11}$, $G_{i/o}$	PLCβ activation, cAMP inhibition	+	+	+	+	+	+	+
P2Y4	UTP (ATP, UDP)	2.5	$G_{q/11}$, $G_{i/o}$	PLCβ activation, cAMP inhibition	ND	+	+	+	+	+	ND
P2Y6	UDP, UTP	0.3 (UDP), 6 (UTP)	$G_{q/11}$	PLCβ activation	+	+	+	+	+	+	ND
P2Y11	ATP	17	G_{s}, $G_{q/11}$	cAMP production, PLCβ activation	ND	+	+	+	+	+	ND
P2Y12	ADP	0.07	$G_{i/o}$	cAMP inhibition	+	+	+	ND	+	+	ND
P2Y13	ADP, ATP	0.06 (ADP), 0.26 (ATP)	$G_{i/o}$	cAMP inhibition	+	+	ND	+	+	+	ND
P2Y14	UDP-glucose	0.1–0.5	$G_{q/11}$	PLCβ activation	+	ND	ND	+	+	+	+
P1 adenosine receptors											
A1	adenosine	0.2–0.5	$G_{i/o}$	cAMP inhibition	+	+	+	+	ND	ND	ND
A2A	adenosine	0.6–0.9	G_{s}	cAMP production	+	+	+	+	+	+	+
A2B	adenosine	16–64	G_{s}	cAMP production	+	+	+	+	+	ND	+
A3	adenosine	0.2–0.5	$G_{i/o}$, $G_{q/11}$	cAMP inhibition, $InsP_3$ generation	+	+	+	+	+	ND	+

Table 1. Purinergic receptors classification. For each receptor it is reported ligands, downstream pathways activated after their stimulation and expression in immune cell types [10].

P2X and P2Y receptors are P2 receptors that differ for pharmacology and downstream signalling pathway they are associated with (Figure 2).

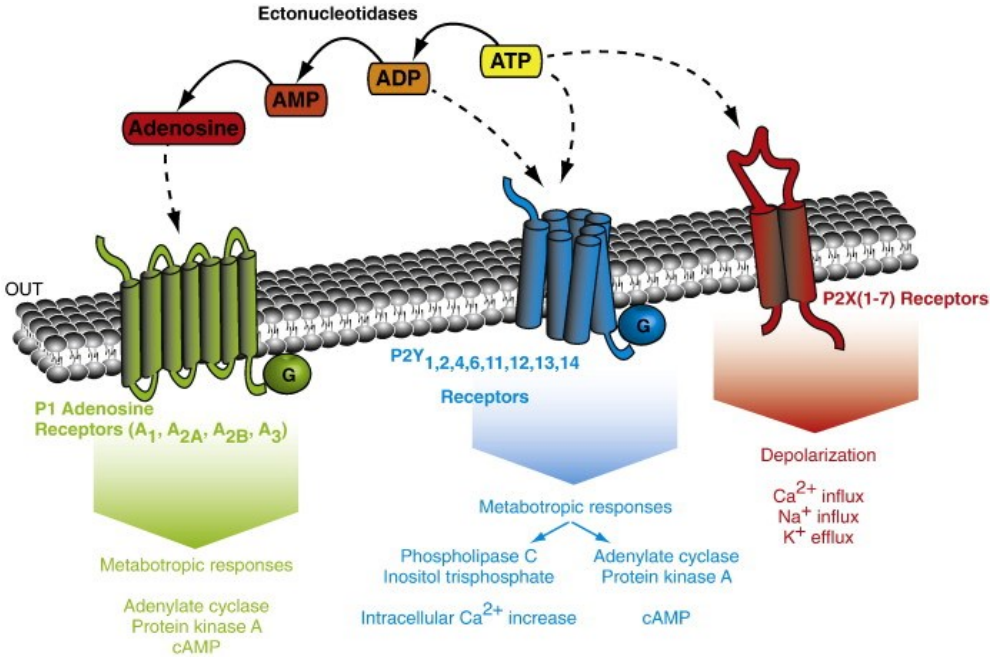

Figure 2. Representation of purine receptors subtypes based on their structure, pharmacology and downstream signalling pathways activated.

The P2Y are seven membrane-spanning (7TM), G protein coupled receptors, for which the activating ligands include ATP and some other purine or pyrimidine di- or tri-phosphate nucleotides such as ADP, UTP or UDP, and their activation initiates signalling pathways dependent on the G-proteins they are coupled to [24].

P2X receptors are physiologically and exclusively activated by extracellular ATP and they are ligand-gated ion channels that modulate membrane permeability for monovalent and divalent cations [25].

P2X receptors

This subfamily is composed of seven members, named P2X1-P2X7, with a membrane topology of two hydrophobic transmembran domains (TM1 and TM2), separeted by a large extracellular loop for the binding of ATP (Figure 3). P2X receptors were proposed to be homo- or in some cases hetero-trimeric [11].This has been confirmed in recent studies performed using X-ray crystallography to solve the three-dimensional structure of the zebrafish P2X4 receptor (Figure 4) [26, 27].

P2X receptors activation mediates very rapid cellular effects, generally resulting in a depolarizing inward current due to a major influx of Na^+ and Ca^{2+} into the cytosol, while a minor but concomitant efflux of K^+ is generate [28].

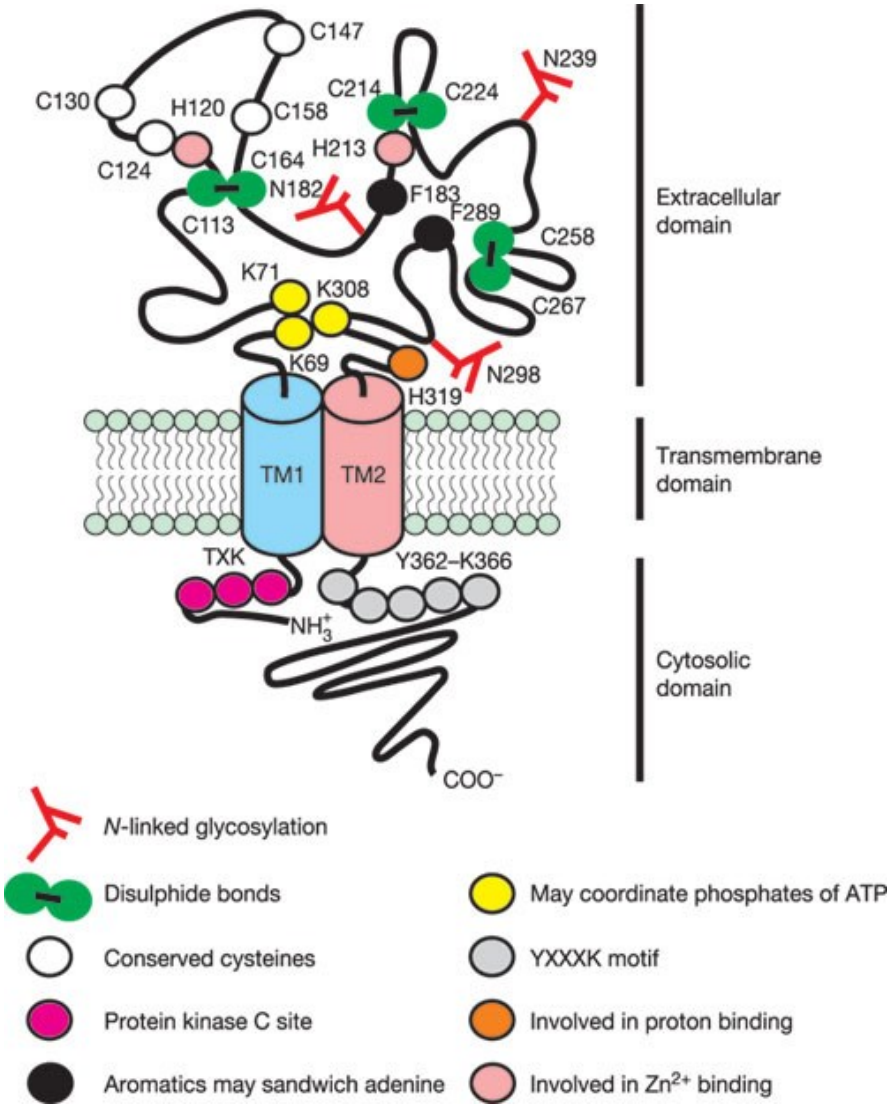

Figure 3. Topology and key features of P2X receptor subunit. This hypothetical view is based mainly on experiments with P2X1 and P2X2 receptors [28].

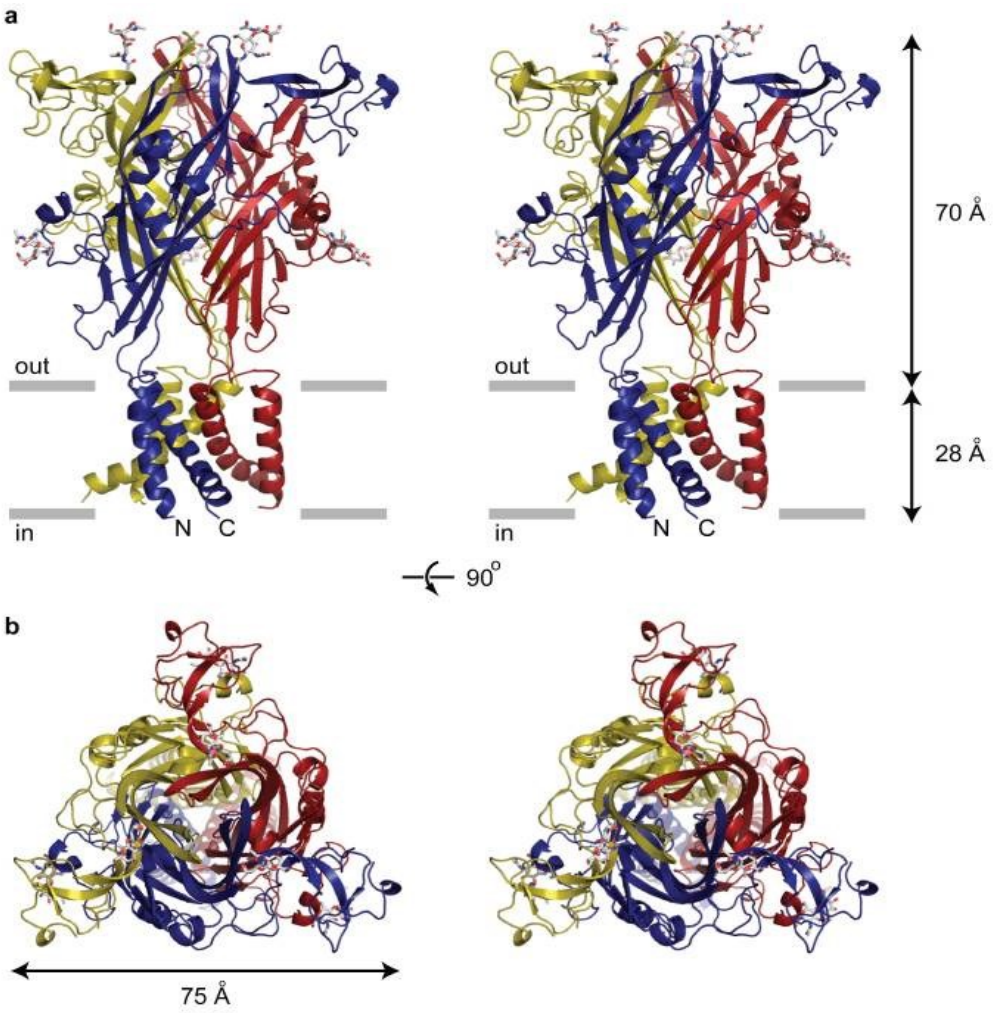

Figure 4. **a**, Stereoview of the homotrimeric the zebrafish P2X4 receptor structure viewed parallel to the membrane. Each subunit is depicted in a different colour. *N*-acetylglucosamine (NAG) and glycosylated asparagine residues are shown in stick representation. The grey bars suggest the boundaries of the outer (out) and inner (in) leaflets of the membrane bilayer. **b**, Stereoview of the homotrimeric zebrafish P2X4 structure parallel to the molecular three-fold axis from the extracellular side of the membrane [26].

P2X7 receptor

Among the members of the P2X receptors family, the P2X7 receptor (P2X7R) is very unique by multiple features, from its molecular structure, to its biophysical and pharmacological properties [29-31]. Unlike the other P2X receptors, P2X7R has an unusually long cytoplasmic C-terminal end, that endows this receptor with the ability to generate a non selective membrane pore, that allows transmembrane fluxes to cations, nucleotides and other small hydrophilic molecules of MW up to 900 Da [30].

Gene, splicing variants and single nucleotide polymorphisms (SNPs)

The human P2X7R is encoded by the *P2RX7* (purinergic receptor P2X, ligand-gated ion channel, 7) gene located on the locus 12q24.31. The *P2RX7* gene comprises 13 coding exons. Ten naturally occurring alternative splicing variants have been identified in humans and have been named P2X7A to J [30, 32]. The P2X7A variant is the well-characterized full-length receptor [31]. Among the ten, five splice variants (P2X7B, P2X7C, P2X7E, P2X7G and P2X7J) are lacking the C-terminal intracellular tail of the receptor. The truncated P2X7B seems to display the same pharmacological properties, towards both agonists and antagonists, as the P2X7A and to be functional as an ion channel, but it is unable to trigger membrane permeabilization for large cationic molecules [33].

The human *P2RX7* gene is highly polymorphic, and numerous single nucleotide polymorphisms (SNPs) have been identified in the last years (Figure 5). While a vast majority of these SNPs are located into intronic sequences, about 150 non-synonymous SNPs (NS-SNPs) have been reported [16]. Some of these variants have drawn a lot of attention and were particularly studied following genetic association analysis, that proposed them as important genetic factors altering the susceptibility of individuals to various diseases [34, 35]. Some of these NS-SNPs are responsible for alterations in functional properties of the human receptor, which were mostly assessed by recording inward currents and/or dye uptake [16].

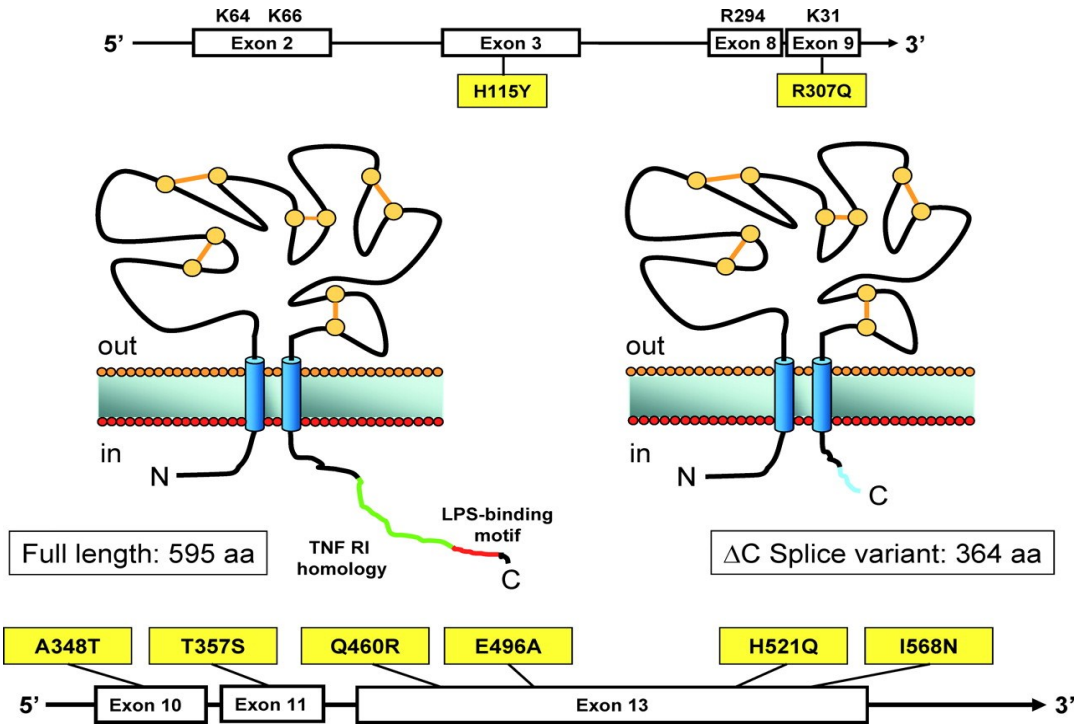

Figure 5. The P2X7R: membrane topology and aa substitutions caused by the main SNPs so far described. The full-length and truncated (ΔC) splice variant of the P2X7R are shown. The truncated form lacks almost the entire COOH tail (249 aa, green, red, and short black traits) but bears an extra 18 aa (light blue trait) due to inclusion of the intron between exons 10 and 11 (94). TNFRI homology domain (green) and putative LPS-binding region (red) are shown. Cysteine residues forming putative disulfide bridges are also shown. Amino acid changes are highlighted in yellow boxes, whereas residues involved in ATP binding in exons 2, 3, 8, and 9 are indicated in black [36].

General structure of the P2X7 receptor

The P2X7 receptor, like other P2X, is functional under a multimeric assembly of three subunits [37, 38]. Each subunit bears a dolphin-like three-dimensional topology as predicted by the X-ray crystallography analyses performed on the zebrafish P2X4 receptor in the closed and ATP-bound open states [26, 27] and subsequent structural modelling [30]. In line with other P2X, the P2X7R subunit consists of a large, glycosylated and cysteine-rich extracellular domain composed of 285 amino acids, two transmembrane-spanning helices called TM1 and TM2 domains, a short intracellular N-terminal domain and an intracellular C terminal domain. One structural particularity of P2X7R, being responsible for multiple functional specificities, is that with 595 amino acid residues the P2X7R protein is significantly bigger than any other P2X subunits. This difference in the protein size is solely due to the C-terminal domain which is longer than those of all other P2X receptors by containing from 70 to 220 more residues [30]. The C-terminus of P2X7R

has been implicated in regulating receptor functions and sub-cellular localization, but also in protein-protein interactions and the initiation of intracellular signalling cascades [39].

P2X7 receptor channel and pore formation properties

P2X7R is the less sensitive receptor for extracellulat ATP, in fact, it requires hundreds of micro moles/liter of agonist to be activated [40].

After ATP stimulation, like all other members of the P2X receptors family, P2X7R opens within milliseconds a transmembrane ion-conducting pathway that is selectively permeable to small cations such Ca^{2+}, Na^{+} and K^{+} [31, 40]. As mentioned above, opening of the P2X7R ion channel can mediate extracellular Ca^{2+} entry into the cell to elevate the intracellular Ca^{2+} concentrations, and also intracellular K^{+} efflux. For ligand-gated Ca^{2+}-permeable ion channels like the P2X receptors including the P2X7R, the ion channel functional properties can be studied using the patch-clamp recording technique to directly measure agonist-induced ionic currents through open channels (e.g.[41]). An alternative and widely-used method is using fluorescent Ca^{2+} indicators, such as Fura-2 or Fluo-4, to monitor agonist-induced increase in the intracellular Ca^{2+} concentrations resulting from extracellular Ca^{2+} influx (e. g. [42]).

The ion channel properties of P2X7R have several biophysical properties that contrast with the other P2X receptors. A unique functional peculiariy of the P2X7R ion channel is that it displays no or little desensitization in the presence of agonist even for several tens of seconds or minutes. P2X7R-mediated currents increase in amplitude upon repeated brief applications or sustained applications of agonists, and this is associated with an increase in the sensitivity to the agonist and was called facilitation [43-45].

As detailed previously, a structural feauture of P2X7R compared to all other P2X members, is the long C-term tail. This characteristic could be responsable for the pore forming ability of P2X7R. The receptor, in fact, is perhaps best known for its capacity to induce a phenomenon called membrane permeabilization, that refers to the formation of large pore that allows passage of large cationic molecules up to 900 Da across the plasma membrane [29, 31] (Figure 6). The large pore appears after the activation of P2X7R for tens of seconds to minutes. This can be demonstrated under more physiological conditions by monitoring progressive efflux of pre-loaded fluorescent dyes, for example, calceine [46], and more commonly, by accumulation of extracellular fluorescent dyes, such as YO-PRO-1 (e.g. [47]) and ethidium (e.g. [48]), inside the cells during receptor activation. The latter is widely referred to as fluorescent dye uptake.

It is also worth mentioning that formation of large pore occurs after activation of some other homomeric or heteromeric P2X receptors, including P2X2, P2X4, P2X2/3 and P2X2/5 [49-51].

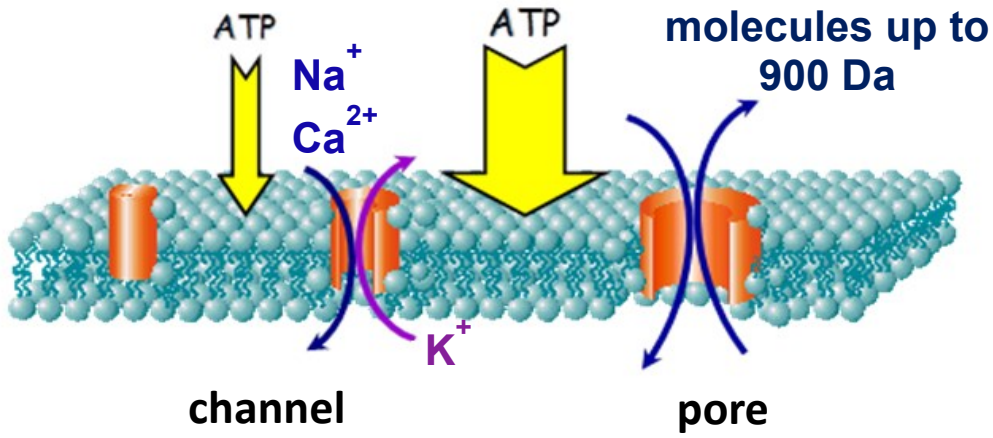

Figure 6. P2X7 receptor stimulation. In presence of ATP, P2X7R mediates Na^+ e Ca^{2+} influx and K^+ efflux through plasma membrane. Repeated stimulation with the agonist or higher concentrations of the same, result in the opening of a pore that allows the passage of molecules up to 900 Da.

P2X7R pharmacology

The preferred P2X7 receptor ligand is ATP, but its activity can be modulated by other pharmacological ATP analogues. 2',3'-(4-benzoil)-benzoil-ATP (BzATP) is the most common P2X7 receptor agonist, but it is not absolutely selective for P2X7R as it can act on P2X1 and P2X3 receptors [52].

Various antibiotics can modulate directly or indirectly P2X7 receptor activity: geldanamycin (GA) has been showed to potentiate P2X7R-dependent response, by binding the amino-terminal ATP-binding pocket of "Heat-Shock" protein 90 (HSP90), thus preventing its interaction with P2X7R itself [53]. Polimixin B, known for its ability to neutralize bacterial endotossin (LPS), potentiates P2X7R stimulation by ATP, thus lowering the cytotoxic threshold of otherwise ineffectual ATP doses [54].

Oxidized ATP (oATP) is largely used as a P2X7R antagonist, even though this covalent reagent is likely to have low selectively, its highly reactive aldehide group can generate a Schiff base with any unprotonated lysine close to any ATP-binding site on the plasma membrane [55-57]. One of the first, potent and selective P2X7R inhibitors was KN-62 [58]. More recently, a family of highly selective and potent KN-62 have been synthesized [59]. A number of medicinal chemistry programmes have led to discovery of several series

of drug-like compounds with distinctive structural properties as highly selective human P2X7R antagonists, with nanomolar potency. Among these there are:

1. A 438079 hydrochloride is a competitive P2X7 receptor antagonist. The compound is devoid of activity at other P2 receptors and possesses antinociceptive activity in models of neuropathic pain *in vivo* [60, 61].
2. A 740003 is a potent, selective and competitive P2X7 receptor antagonist (EC_{50} values are 18 and 40 nM for rat and human respectively). This compound displays selectively over a variety of P2X and P2Y receptors up to concentration of 100 μM. Nevertheless, it reduces nociception in animal models of persistent neuropathic and inflammatory pain [62, 63].
3. AZ 10606120 dihydrochloride is another potent P2X7 receptor antagonist. Differently from those described in advance, AZ 10606120 binds in appositive cooperative manner to sites distinct from, but coupled to, the ATP binding site and acts as a negative allosteric modulator [64, 65].
4. AZ 11645373 is also available to selectively antagonize P2X7 receptor, without effecting all the other P2X subtypes. It inhibits BzATP mediated calcium influx and ATP mediated IL-1β release *in vitro* [66].

P2X7 receptor distribution and biological effects

P2X7R is widely distributed throughout the mammalian body [67]. This receptor was originally thought to be restricted to cells of the hematopoietic lineage, including macrophages, dendritic cells, monocytes, lymphocytes, and erythrocytes, as well as osteoclasts, mast cells, and eosinophils. However, it is now evident that P2X7R is present on cells from other lineages, including osteoblasts, fibroblasts, endothelial cells, and epithelial cells. Furthermore, P2X7R is present on cells in the central and peripheral nervous systems, including microglia, astrocytes, oligodendrocytes, and Schwann cells [68]. In addition, there are reports of the presence of P2X7R on some populations of neurons, including those from the spinal cord, cerebellum, hypothalamus, and substantia nigra [69, 70].

As anticipated before, P2X7 receptor is most expressed in immune cells coming from the hematopoeitic lineage, in which participation of the receptor in the immune response has been extensively documented. Particularly, the contribution of P2X7R is critical in the inflammation by inducing the activation of the inflammasome NLRP3 and caspase-1 with the subsequent release of the proinflammatory citokyne, IL-1β from Pathogens Associated

Molecular Patterns (PAMPs)-primed macrophages and microglial cells [71, 72]. In addition, variuos and numerous cell type-specific signaling pathways have been associated with P2X7R activation. These include the formation of reactive oxygen and nitrogen species and the formation of phagolysosomes and subsequent killing of intracellular pathogens [73-75]. Activation of P2X7R can also lead to a number of membrane-related changes including membrane blebbing, microparticle and exosome release, multinucleated cell formation, reversible phosphatidylserine exposure, and the activation of membrane metalloproteases resulting in the shedding of cell-surface molecules [70, 76]. Recent work has identified additional cell surface molecules shed or release after activation of P2X7R. This includes chemokines [77], adhesion molecules, soluble amyloid precursor protein, prostanoids and various enzymes [35].

P2X7R is a non-desensitizing receptor and this lack of desensitization generates a reversible plasma membrane pore. However, prolonged activation of P2X7R unavoidably leads to cell death [78]. This is the reason why P2X7R has, in general, been linked to cytolytic cell death.

P2X7R and cell proliferation

P2X7R is historically known for its ability to induce cell death through apoptosis [79-81]. A role in cell proliferation would seem to be at odds with this, but evidence suggests that in certain cell types, activation of P2X7R is more likely involved with proliferation than cell death. In T cells, release of autocrine ATP during cell activation through the T-cell receptor, activates P2X7R and enhances secretion of the T cell growth factor IL-2, through stimulation of the nuclear factor of activated T-cells transcription factor (NFATc-1) [82]. Baricordi and colleagues (1996) first suggested a role for P2X7R in mitogen-induced T-cell proliferation. The same group subsequently went on to show that transfection of cell lines with full-length P2X7R or the truncated splice variant increased cell proliferation, especially in the absence of serum [48, 82, 83]. In microglia, pharmacological blockage of P2X7R or overexpression of a receptor pore-mutant (G345Y) to abolish secondary permeability, reduced the proliferative rate. [47, 84].

In B-leukemic lymphocytes, P2X7R stimulation caused a large increase in intracellular Ca^{2+}, while its blockade stopped proliferation. These findings were later extended to HEK293 cells (Human Embryonic Kidney), a cell line lacking endogenous P2X7R. Also, in this cell type, transfection of P2X7R conferred a growth advantage as in other model systems shown previously [83]. In this model faster growth of P2X7R-transfected cultures

depended on both a higher proliferation rate, decreased apoptosis and a high level of activated transcription factor NFATc1. Enhanced trophism of HEK293-P2X7R transfected cells was likely because of the higher intracellular ATP content, which in turn depends on a more efficient mitochondrial metabolism, and a concomitant stimulation of aerobic glycolysis [85]. These cells also showed a higher capacity to invade Matrigel, a parameter that is taken as an index of metastatic potential.

P2X7 receptor in cancer cells

Since the accumulation of information about P2X7R involvment in cell proliferation started to buid up, its possible role in cancer has been hypothisized.

P2X7R was found to be expressed in cancer biopsies (see Figure 7) and cancer cell lines. Several solid tumours have been shown to express the P2X7R, those include breast [86] prostate [87], colon [88], renal [88], cervical cancers [89], neuroblastoma [19, 90], melanoma [91] and papillary thyroid carcinoma [92]. A loss of function polymorphism of P2X7R was also associated to reduced aggressiveness and metastatic dissemination in prostate cancer [93]. Conversely to what observed in other cancer types, P2X7R expression was down modulated in adeno and cervical squamous carcinomas [89, 94]. However, in the same type of cancer a loss of function splice variant of P2X7 receptor (P2X7J) was reported to be overexpressed [95]. Therefore, the presence of other truncated forms of P2X7R associated to increased cell proliferation [48] can not be excluded. Moreover P2X7R was overexpressed by haematological malignancies such as aggressive variants of B-CLL [96] and paediatric acute leukemia [97].

Proof of concept of P2X7 receptor active role in tumor growth was given in 2012 when in an *in vivo* study Adinolfi and colleagues clearly demonstrated a connection between P2X7R expression and tumor growth [88]. Transfection of P2X7R in cells that naturally does not express it, such as HEK293 human embryonic kidney cells or CT26 colon carcinoma cells caused an increase in tumor engraftment and growth. Consequently, silencing or pharmacological blockade of the receptor in P2X7R-endogenously-expressing murine models of neuroblastoma and melanoma caused tumor regression [88]. P2X7R expressing tumors had a thick vascular network and stained positive for VEGF [88, 98]. Pharmacological blockade or silencing of P2X7R reduced VEGF release and vessel formation [88], thus confirming receptor participation in tumor associated angiogenesis.

P2X7 receptor activation has also been involved in the spreading of tumor cells from primary tumor site [98, 99]. In fact, P2X7R promotes cell release of different proteolytic

enzymes such as cathepsins and matrix metalloproteinases [99-101]. Recently, it was reported that P2X7R activation enhanced breast and lung cancer cells invasiveness, through not only protease release but also acting at cytoskeletal remodeling [99, 102, 103]. In human lung cancer cells, P2X7R mediated TGF beta-dependent actin reorganization and migration [102]. In a pancreatic ductal adenocarcinoma cells P2X7R modulator AZ10606120 significantly reduced cell migration [104]. Moreover, P2X7R pharmacological blockade impaired breast cancer cell dissemination in a zebra-fish model of metastasis [99, 103]. These findings imply that P2X7 receptor not only promotes tumor growth but is also involved in metastases development. Thus, P2X7R blocking drugs could be employed as anti tumoral and metastatic agents, as suggested by good results of *in vivo* experimental models [103].

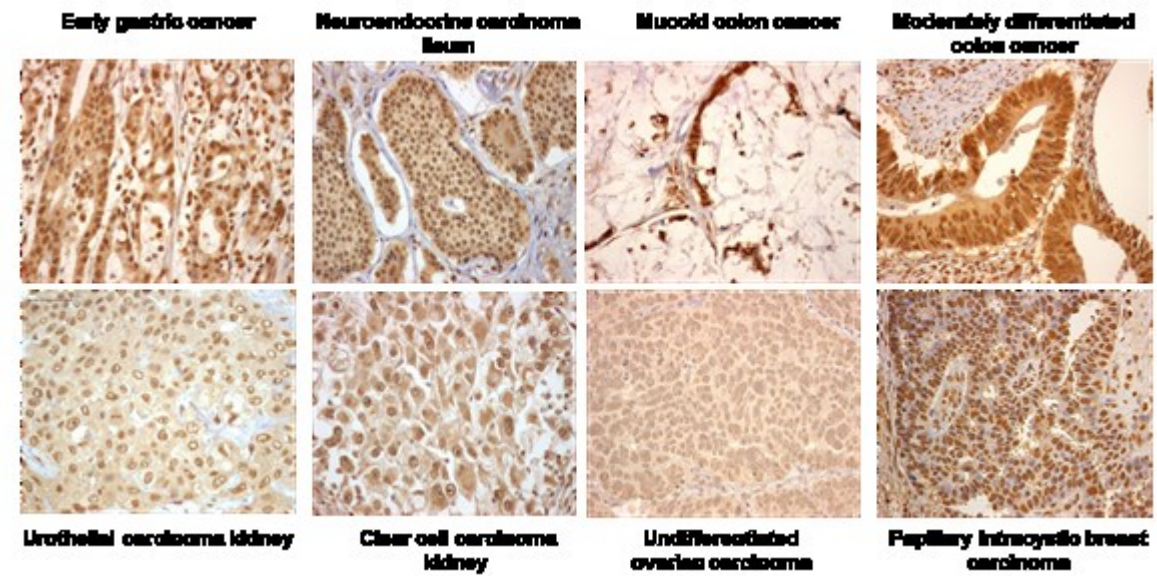

Figure 7. Human cancers express P2X7R. Human tumor specimens were stained with anti-P2X7R antibody [88].

P2X7 receptor in immune response and in tumour-associated immune cells

Tumours are infiltrated with different subsets of immune cells and some tumors originate from a chronic inflammatory environment, thus there is a well-orchestrated functional interaction among infiltrating inflammatory cells and the tumour [105, 106]. P2X7R is highly expressed and controls the function of different immune cells such as monocytes, macrophages, dendritic cells and lymphocytes [15, 107, 108]. As detailed in the previous

section, tumor microenvironment presents high levels of extracellular ATP and therefore activation of the P2X7R is likely to occur in cancer cells expressing the receptor and in immune cells infiltrating tumour.

The P2X7R is a focus of increasing interest for its ability to modulate the immune response [22]. The effects of P2X7R on the immune response likely occurs at multiple levels: at the level of tumor Ag presentation to $CD4^+$ T lymphocytes by DCs; of DCs stimulation by DAMPs, chiefly ATP, released by the tumor cells themselves; at level of pro-inflammatory cytokine release, and probably also at the level of inflammatory cell recruitment [109, 110].

In the tumour environment dying tumour cells, e.g. after chemotherapy treatment, increased the activation of P2X7R in macrophages and dendritic cells via the release of ATP (Figure 8). This release of ATP in conjunction with Toll-like receptor (TLR) engagement with other DAMP signals, such as the high-mobility group protein 1 (HMGB1), are essential to elicit a proper anti-cancer immunity [110, 111]. In macrophages and dendritic cells, the activation of these pathways converges in the assembly of the inflammasome, a central innate immune sensor for PAMPs and/or DAMPs [71, 112, 113]. The NLRP3 inflammasome activated via P2X7R, has been described as being responsible for eliciting $CD8^+$ T-cell mediated cancer eradication following anticancer treatments [110, 114].

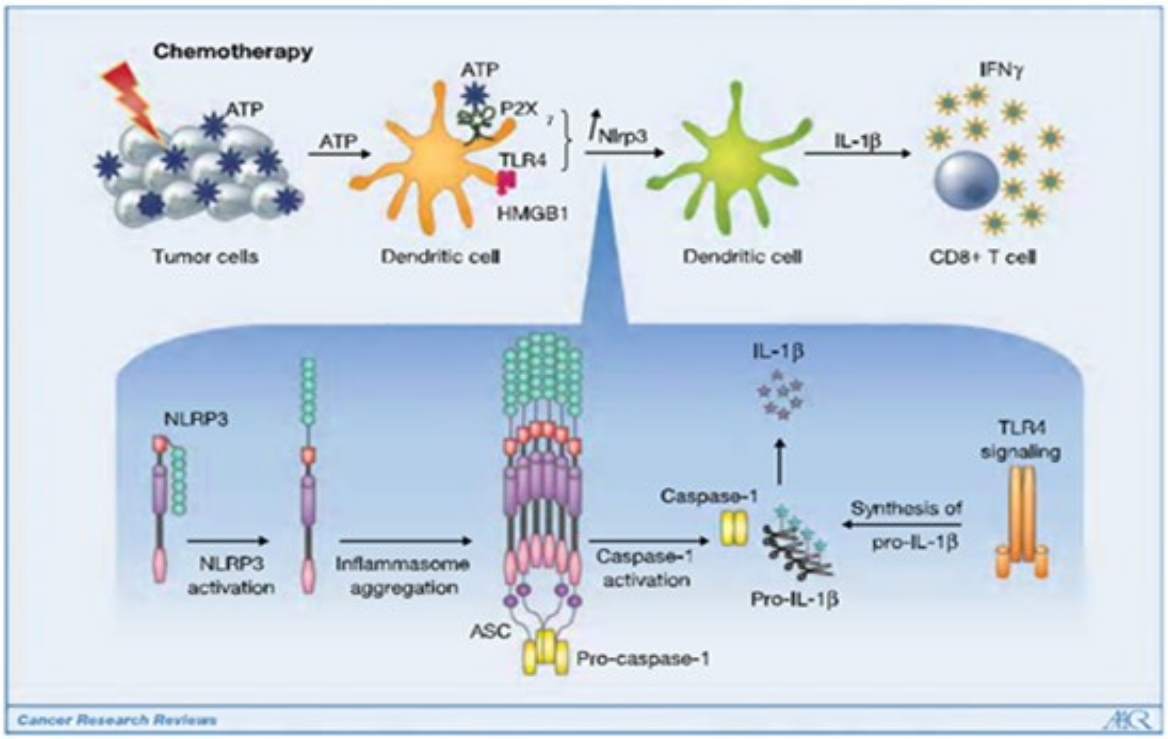

Figure 8. The integrity of the NLRP3 inflammasome is required for IFNγ polarized $CD8^+$ T-cell response with dying tumor cells. During a hit with chemotherapy, dying tumor cells are captured and processed by

host DCs triggering a tumor-DCs crosstalk dictated by ATP/P2X7R and HMGB1/TLR4 molecular interactions. ATP and HMGB1 act in concert to ignite the NLRP3 inflammasome in DCs, culminating in IL-1β processing and secretion in the extracellular milieu. IL-1β then contributes to the TCR-driven IFNγ polarized $CD8^+$ T-cell response, a mandatory step for the efficacy of chemotherapy [110].

As seen before, P2X7R antagonism might be a promising route for the treatment of tumors expressing this receptor, but in view of P2X7R role in anti-tumor immune response, receptor blockade might in the end be detrimental to the host by impairing anticancer defence. In this regard, Idzko and co-workers recently showed that during graft-versus-host-disease (GVHD) inflammation was severely curtailed in mice deleted of the *p2x7* gene, despite the massive release of ATP observed at the target organ (intestine) [115]. Moreover pharmacological P2X7R blockade prevents rejection in an allogeneic heart or pancreatic insulae transplantation models [116, 117] .

Considering a tumor as an allogenic transplant, these data suggest that expression of the P2X7R by host immune cells might critically affect tumor-host interactions, and with P2X7R active on both the tumor and the host cells, receptor blockade might have final outcome difficult to anticipate.

AIM OF THE WORK

The P2X7R is a potent pro-inflammatory receptor participating in transplant rejection and anti-tumor immunity. On the other hand, recent data show that P2X7R expression by tumor cells enhances tumor growth and metastatic spreading. Several potent and selective P2X7R blockers, currently in clinical trials for the treatment of chronic inflammatory diseases, have been developed. However, use of P2X7R-targeting drugs in cancer therapy is not straightforward since the role of host P2X7R in anti-cancer defence has not been explored so far.

With this study we want to explore the effects of genetic deletion of host P2X7R on tumor growth and metastatic spreading, and the final outcome of systemic administration of P2X7R blockers in P2X7R-wt mice bearing tumor.

Our work wants to clarify to what extent host P2X7R is needed to control tumor growth, and whether P2X7R blockade might be in the end a novel avenue to fight cancer.

Data presented in this work are part of the results that were published on Cancer Reasearch in “Accelerated tumor progression in mice lacking the ATP receptor P2X7” [118].

MATERIALS AND METHODS

Reagents and antibodies

Tris base, sodium chloride, Triton X-100, RPMI, non essential aminoacidics, hygromycin, haematoxylin, eosin, ethanol, Bouin fixative solution, Cell dissociation solution, rabbit polyclonal anti-P2X7 antibody (P8232) were acquired from Sigma-Aldrich (Milan, Italy). FBS, penicillin and streptommycin solution were from Euroclone (Milan, Italy). H_2O_2 and xylene were from Carlo Erba (Rodano, Italy). 3,3'-diaminobenzidine (DAB) chromogen solution, Target Retrieval solution pH 9 (10x), horse radish peroxidase (HRP)- conjugated goat anti-rabbit were purchased from Dako (Dako Italia, Milano, Italy). Anti-F4/80 (CI:A3-1), sheep anti-rat HRP-conjugated IgG, and TransIT-2020 transfection reagent were from Tema Ricerca (Bologna, Italy). Rabbit polyclonal anti-CD3 (ab5690) and anti-VEGF (ab46154) and rat monoclonal (ab22378) anti-CD8 Abs were from Abcam (Cambridge, UK), whereas mouse VEGF and mouse IL1β/IL-1F2 Quantikine® ELISA kits were from R&D systems (Minneapolis, MN, USA). AZ10606120 dihydrochloride and A74003 were acquired from Tocris Bioscience (Bristol, UK). Red blood cell lysis buffer was from Sigma-Aldrich, while Recombinant Murine (rm) GM-CSF was from PeproTech (London, UK). The intracellular luc2 luciferase expression vector carrying a hygromycin resistance (pGL4.50/hygro) was from Promega (Madison, WI, USA). The P2X7shRNA in pSuper.neo.GFP vector was a kind gift of Dr. Diaz-Hernandez (Universidad Complutense, Madrid, Spain [119].

Cell cultures and transfections

B16 melanoma and CT26 colon carcinoma cells were a kind gift of Drs. M.P. Colombo (Istituto Nazionale Tumori, Milano) and Guido Kroemer (INSERM, Paris, France), respectively, and extensively tested in the authors' laboratories [120, 121]. The N13 microglial cells was a kind gift of Dr. Paola Ricciardi-Castagnoli (Singapore Immunology Network, Singapore), and extensively tested in the authors' laboratory for cytokine and surface markers expression [109].

B16, CT26 and N13 cells were grown in RPMI medium supplemented with non-essential aminoacids, containing 10% FBS, 100 U/ml penicillin and 100 mg/ml streptomycin. Cells were detached with the Cell dissociation or Trypsin solutions (Euroclone, Italy), plated in

75cm^2 Falcon flasks (Microtec, Naples, Italy) and incubated at 37°C in humidified incubator in the presence of 5% CO^2.

All transfections were performed with TransIT-2020 transfection reagent as per manufacturer's instructions. Briefly, 1.5×10^6 B16 cells were plated in Petri dishes 18-24 hours day before transfection such that they reach high confluence (~60-80%) at the time of transfection. The next day purified plasmid DNA (10 μg) was mixed with TransIT reagent in 1 ml of serum-free medium and incubate at room temperature for 30 minutes. Then the TransIT transfection reagent-DNA complexes solution was dropwise added to cells, whose medium was first replaced with serum-free medium. The day after cells were refreshed with complete medium, in order to wash away the excess of transfection reagent-DNA complexes. Stably transfected cell lines were obtained starting from 48-72h after transfection by selection with either hygromicyn (0,1-0,2 mg/ml) or G418 sulfate (0.2-0.8 mg/ml) (Calbiochem, La Jolla, CA, USA). B16shRNA single cell-derived clone was obtained by limiting dilution starting from the polyclone.

Real-Time PCR

Total mRNA was extracted with TRIzol® RNA Isolation Reagent and the PureLink RNA Mini Kit (Life Technologies, Foster City, CA, USA), according to manufacturers' instructions. Quantitative RT-PCR was performed with the High-Capacity cDNA Reverse Transcription Kits (Applied Biosystems, Foster City, CA, USA). Samples were run in duplicate in an AB StepOne Real Time PCR (Applied Biosystems) with TaqMan Gene Expression Master Mix (Applied Biosystems) using the following primers: Mm00440578m1 (murine P2X7 receptor, mP2X7R) and 4352339E (mouse glyceraldehyde 3-phosphate dehydrogenase, mGAPDH).

Western Blot

Proteins were analyzed on Bolt Mini Gels 4–12% SDS-PAGE (Life Technologies) and transferred onto nitrocellulose paper (GE Healthcare Life Sciences, Milano, Italy). Membranes were blocked with 2% nonfat milk (Bio-Rad, Hercules, CA, USA) and 5% bovine serum albumin (Sigma-Aldrich) in TBS-T buffer (10 mM Tris-HCl, 150 mM NaCl, pH 8.0, and 1% Tween-20) and probed overnight at 4°C with rabbit anti-P2X7R (1:200 dilution; Sigma-Aldrich) or rabbit anti-actin (1:1000 dilution, cat. no. A2668; Sigma-Aldrich) antibodies. Membranes were washed 3 times for 5 min with TBS-T buffer and

incubated in the same buffer for 2 hours at room temperature with horseradish peroxidase-conjugated secondary polyclonal antibody goat anti-rabbit (1:500 dilution, cat no. ab7090; Abcam). After washing with TBS-T buffer, proteins were detected using ECL reagent (GE Healthcare Life Sciences). Gray values were quantified with ImageJ software.

Measurement of intracellular calcium concentration ($[Ca^{2+}]_i$)

Changes in the cytosolic free Ca^{2+} concentration were measured in a thermostat controlled (37°C) and magnetically stirred Cary Eclipse Fluorescence Spectrophotometer (Agilent Technologies, Cernusco SN, Milan, Italy) with the fluorescent indicator fura-2/acetoxymethyl ester (fura-2/AM) as previously described in [83]. Briefly, 2×10^6 cells were loaded with 2 μM fura-2/AM for 30 min in the presence of 250 μM sulfinpyrazone in saline solution (125 mM NaCl, 5 mM KCl, 1 mM $MgSO_4$, 1 mM NaH_2PO_4, 20 mM HEPES, 5.5 mM glucose, 5 mM $NaHCO_3$, and 1 mM $CaCl_2$, pH 7.4), rinsed, and re-suspended at a final concentration of 10^6/ml in the same buffer. Excitation ratio and emission wavelength were 340/380 and 505 nm, respectively.

Cell proliferation assay

Cell proliferation was assessed by direct cell counting. 5×10^3 cells/well were plated in Falcon 6-wells plates and left adhere completely. Incubation media was not replace up to 72 hours. Pictures were taken every 24 hours, five random photographs per well were acquired with Olympus IMT-2 (Olympus Corporation, Tokio, Japan) microscope equipped with a 20× phase contrast objective. Cells were then counted with ImageJ software (Wayne Rasband, NIH, Bethesda, USA). Proliferation rate was expressed as fold increase over time zero.

Mice strains, tumor generation, *in vivo* imaging and drug administration

In vivo experiments were performed with two different *p2x7*$^{-/-}$ mouse strains and corresponding wt controls: C57Bl/6 were a gift from GlaxoSmithKline and BALB/cJ previously obtained in Dr. Jorgensen laboratory [122]. Mice were housed under controlled conditions of temperature (22±2 °C) and humidity (55±5 %), fed *ad libitum*, until used. To induce primary tumor formation 5×10^5 B16, P2X7R silenced B16 or 2.5×10^5 CT26 cells were re-suspended in 100 μl of sterile PBS and inoculated into subcutaneous fat of the right limb of syngeneic C57Bl/6 or BALB/cJ mice, respectively (n = 6 for each condition).

Within 5-7 days from the *inoculum*, tumor masses became detectable by palpation and visual inspection, with a volume range from 10 to 30 mm^3. Tumor size was measured with a manual caliper, and the volume calculated approximating the tumor mass to an ellipsoid, according to the following equation: volume = $\pi/6$ [w1 x $(w2)^2$], were w1= major diameter and w2= minor diameter. Before the appearance of clear signs of discomfort, mice were anesthetized and sacrificed by cranial-cervical dislocation. Tumor masses were *post-mortem* excised, measured with a caliper and photographed. Every sample was cut in two almost equal parts that were either fixed in Bouin or kept at -80°C for further analysis. Blood samples were obtained by *post mortem* beheading. Intracellular luciferase photon emission was followed with a total body luminometer (IVIS Lumina, Caliper-Perkin Elmer, Hopkinton, MA, USA). Briefly, mice were anesthetized with 2.5% isofluorane and intraperitoneally injected with 150 mg/kg D-luciferin (Caliper, Perkin Elmer). After 15 minutes, necessary to guarantee complete luciferin bio-distribution, luminescence was captured from dorsal and ventral views. Bioluminescence was quantified as total photon emission using the Living Image® software (Caliper-Perkin Elmer). Lung metastasis was obtained by intravenous (i.v.) injection of 5×10^5 wt B16 or melanoma cells into the caudal vein of syngeneic C57Bl/6 mice.

For P2X7R antagonists administration, C57/Bl6-wt mice were divided into 3 groups and treated with AZ10606120 (300 nM, n=6), A74003 (10 μM, n=6), or placebo (sterile PBS containing 0.005% DMSO, n=6). Treatments were administrated as a 100 μl intraperitoneal injection every two days after first tumor mass detection. Tumor mass size was measured by manual caliper as described before. All animal procedures were approved by the University of Ferrara ethic committee and the Italian Ministry of Health in compliance with international laws and policies (European Economic Community Council Directive 86/109, OJL 358, Dec. 1, 1987, and NIH Guide for the Care and Use of Laboratory Animals).

Bone marrow transplantation and tumor growth in P2X7R-wt and P2X7R-KO mice

P2X7R-wt and P2X7-KO mice on a BALB/cJ background were treated with Treosulfan (Medec Gmbrl; 1.5 g/kg/d) for 3 consecutive days. Treosulfan was used as a single agent for conditioning before bone marrow transplantation (BMT) to achieve myeloablation as described [123]. Recipient mice were i.v. injected with 1×10^7-nucleated cells obtained from P2X7R-wt or P2X7-KO donors. Bone marrow cells were obtained by flushing the

cavity of freshly dissected femurs with sterile 0.9% NaCl saline solution. Cells were dispersed by pipetting, washed, counted, and re-suspended in saline and i.v. injected, as described by Sangaletti and colleagues [124]. To verify engraftment, peripheral blood mononuclear cells withdrawn from the retro-orbital sinus 6 weeks after BMT were resuspended in TRIzol® RNA Isolation Reagent for RNA isolation and evaluated for P2X7R expression by quantitative RT-PCR. Eight weeks after BMT, mice were subcutaneously inoculated in the right hip with CT26 murine colon carcinoma cells (2.5×10^5 cells/mouse).

ELISA assays

Mouse blood was harvested in tubes containing 8% EDTA, and plasma collected after centrifugation (1000 x *g*, 10 min at 4° C). Tumor specimens were homogenized in lysis buffer (300 mM sucrose, 1 mM K_2HPO_4, 5.5 mM D-glucose, 20 mM Hepes, 1 mM phenylmethylsulfonyl fluoride, 1 mM benzamidine, 0.5% IGEPAL) with a Potter pestle. Plasma samples and tumors homogenates were then assayed for IL-1β and VEGF content with appropriate anti-mouse Quantikine® Elisa kits (R&D Systems) as per manufacturer's instructions. Total amount of VEGF release from B16 or B16shRNA cells *in vitro* were assessed as detailed below: 2×10^5 cells were seeded into 24-well culture dishes in complete RPMI medium, left to adhere and further incubated for 24 hours in serum–free medium. After this time, supernatants were withdrawn and assayed for VEGF levels as seen before. Cell culture supernates and tumor homogenates were diluted where needed before Elisa quantification and intramass cytokine content where normalized on total amount of protein, estimated with Bradford quantification.

Isolation of bone marrow-derived DCs from WT and P2X7R KO mice

Bone marrow-derived cells were obtained as previously described in [125, 126]. Briefly, tibiae and femurs from 6-weeks-old P2X7R-wt and P2X7R-KO mice were removed and cleaned from the surrounding muscle tissue by rubbing with tissue paper. Intact bones were left in 70% ethanol for 2–5 min for disinfection, then both ends were cut with scissors and the marrow flushed with 1 ml of RPMI medium using a sterile syringe. The cell suspension was collected and washed with RPMI medium by 10 min centrifugation at 1100 rpm. Cells were then incubated for 5 min at room temperature in 2 ml of red blood cell lysis buffer (Sigma-Aldrich). Reaction was stopped by adding 15 ml of RPMI medium, cells were

centrifuged, re-suspended in rm-GM-CSF-supplemented (20 ng/ml) RPMI medium, counted and seeded in Petri dishes at a concentration of $2.5x10^5$ cells/ml. At day 3, 6 and 8 half of the medium was withdrawn and replaced with fresh rm-GM-CSF-containing medium. At day 10 DCs were collected, counted and seeded at a concentration of 10^5 cells/ml in the presence or absence of 10^5 B16 wt cells/ml. Supernatants were collected after 24h of co-culture and assayed for IL-1β content by ELISA, as described before.

Histology and immunohistochemistry

Excised tumor masses were fixed in Bouin's fixative for 7 hours at 4 °C, dehydrated in cold-graded ethanol series, cleared in xylene and embedded in paraffin. Serial 7 µm-thick sections were stained with haematoxylin and eosin (H&E) for general histology. For the immunohistochemistry (IHC) of CD3, F4/80 and VEGF, sections were rehydrated, washed in Tris-buffered saline (TBS, 150 mM NaCl supplemented with 50 mM, Tris pH 7.6), blocked for 1 hour at room temperature in TBS containing 10% FCS and 1% BSA, incubated for 16 hours at 4°C with TBS containing 1% BSA and the diluted primary antibodies (anti-CD3 or anti-VEGF rabbit polyclonal antisera, both at 1:100, or the anti-F4/80 rat mAb 1:80, and CD8 1:50). For IHC detection of CD8, before incubation with primary antibody, it was performed heat induced epitope retrieval using Dako Target Retrieval solution. Slides were then washed twice in TBS containing 0.025% Triton X-100, and endogenous peroxidase activity was blocked by a 20 min incubation at room temperature in 0.3% H_2O_2-containing TBS. After several rinses in TBS, sections were incubated for 1 hour at room temperature with 1% BSA-containing TBS, and the diluted secondary antibodies (HRP-conjugated goat anti-rabbit IgG, 1:200, or sheep anti-rat IgG, 1:1000). Tissue sections were then washed twice in TBS, and peroxidase activity detected by a 6-10 min incubation at room temperature with Liquid DAB Substrate Chromogen System (Dako). When appropriate, nuclear counterstaining was performed with Mayer's hematoxylin. Sections were dehydrated, mounted with EUKITT (Kindler GmbH, Freiburg, Germany), and images acquired and analysed with a Nikon eclipse 90i digital microscope equipped with a NIS-elements software (Nikon Instruments Europe, Anstelveen, The Netherlands).

Wound healing Assay

N13 and N13R migration was investigated by wound healing assay. Briefly, N13 and N13R cells were seeded in Petri dishes at a concentration of 2.5 x 10^5/ml, placed in a CO_2 incubator (37°C), allowed to reach confluence and scratched with a sterilized one-milliliter pipette tip to generate wounding across the cell monolayer. Cell migration was observed in a sealed and thermostatic (37°C) chamber, at controlled CO_2 concentration (5%), across a wound spanning 100 µm. Images were then acquired for 16 hours using a Nikon Swept Field Confocal system (Nikon instruments, Melville, NY, USA), at 20× magnification under transmitted light. Images were then analyzed using open source ImageJ Fiji software.

Statistics

Unless otherwise stated, data are shown as mean ± SE of the mean. Test of significance was performed with Student's T test using Graphpad InStat (GraphPad Software Inc, San Diego, CA, USA).

RESULTS

Accelerated growth of subcutaneous tumors in P2X7R-KO mice

It has been shown that lack of expression of the P2X7R prevents GVHD [115] and that P2X7R targeting in mouse increases long-term survival of heart transplants and delays pancreatic islets graft rejection [116, 117]. On the basis of these observations we hypothesized that host P2X7R deletion might facilitate tumor engraftment and progression. To investigate host-tumor interaction in the P2X7R-deleted host, we used B16 mouse melanoma and CT26 mouse colon carcinoma cells.

B16 melanoma model in syngeneic C57black/6 mice

B16 melanoma cell were subcutaneously injected in syngeneic C57black/6 mice. Lack of P2X7R did not affect B16 melanoma cells engrafting, as it occurred in all instances in both P2X7R-KO and wt mice. Tumor growth, assessed by calliper, was barely measurable up to post-injection (p.i.) day 6 in both wt and P2X7R-KO mice. After p.i. day 9, tumors reached a size amenable to calliper measurement, and it became clear that growth kinetic was much faster in the P2X7R-deleted than in the wt host, leading to a tumor mass that was about three fold as large in the KO than in the wt host (Figure 9A). Size difference between tumors grown in the two mouse strains was confirmed at *post-mortem* analysis at p.i. day 14 (Figure 9B, upper panel).

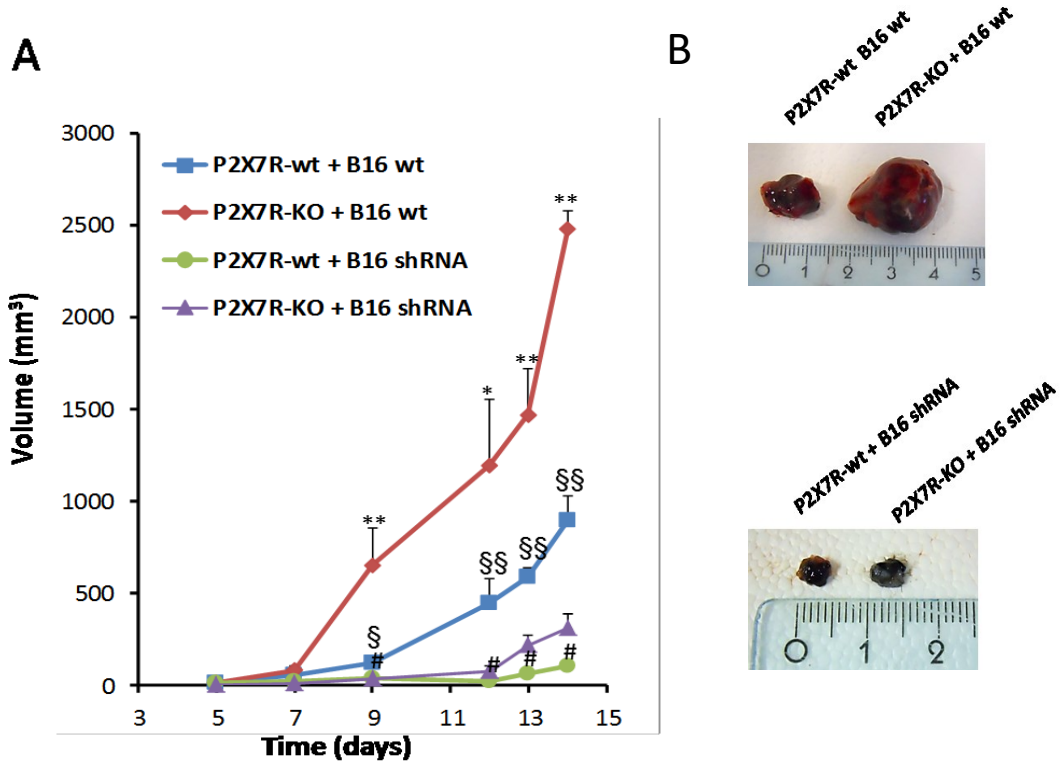

Figure 9. Accelerated growth of B16 melanomas in C57Bl/6 P2X7-KO mice. **A**, C57Bl/6 mice (n = 6) were subcutaneously inoculated into the right hind leg either with B16 cells (5×10^5) stably transfected either with cytosolic luciferase (cytLuc) alone, or with both cytLuc and P2X7R shRNA. Tumor volume was in vivo assessed by calliper measurement at the indicated time points. Data are average ± SEM. *, $p < 0.05$; **, $p < 0.01$ versus P2X7R-wt+B16-wt; §, $p < 0.05$; §§, $p < 0.01$ versus P2X7R-wt+B16-shRNA. #, $p < 0.05$ versus P2X7R-wt shRNA. **B**, Representative pictures of P2X7R-expressing (top) or P2X7R-silenced (bottom) tumors from wt or P2X7R-KO mice at post-injection day 14.

In a previous work we demonstrated that expression of the P2X7R by transplanted tumors had a pronounced growth-promoting effect both in the immunodepressed and in the syngeneic immunocompetent host [88]. To test whether P2X7R expression by the tumor cells might affect tumor growth in the P2X7R-deleted host we generated stable P2X7R-silenced (P2X7R-shRNA) B16 cell clones. Silencing of P2X7R with short harpin RNA in B16 cells caused strong reduction in protein expression, as shown by Western blot, and in receptor functionality (Figure 10A and B), as the Ca^{2+} concentration changes evoked after receptor stimulation was three fold lower in P2X7R-silenced B16 cell clones compared to wt (Figure 10C and D). Downregulation of P2X7R reduced also cell proliferation rate *in vitro*, as expected (Figure 10E).

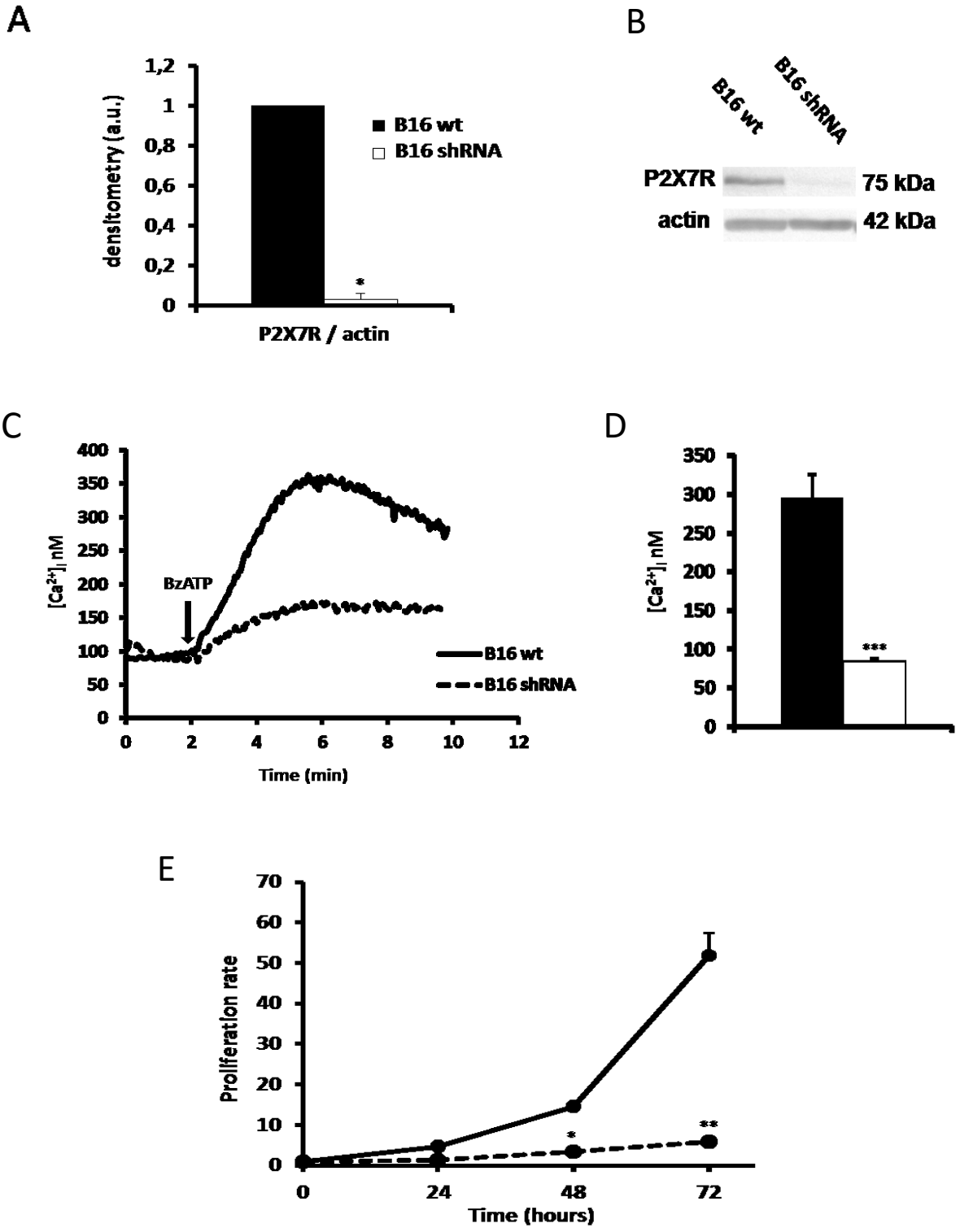

Figure 10. Characterization of P2X7R shRNA B16 cells. **A**, densitometry of P2X7R protein expression. *B*, representative Western blot. **C**, Fura-2 measurement of 200µM Benzoyl ATP (BzATP)-triggered intracellular Ca^{2+} increase. **D**, Averages intracellular Ca^{2+} increases in wt and P2X7R-silenced B16 cells. Data are averages ± SEM, n = 5. ***, $p < 0.001$. **E**, proliferation rate of wt and P2X7R-silenced B16 cell cultures.

As regards *in vivo* experiments, Figure 9A shows that silencing tumor P2X7R caused a profound inhibition of tumor growth, independently of the host *p2x7R* genetic background. Tumor masses generated by P2X7R-silenced B16 cell clones were barely detectable in both the P2X7R-KO and wt host up to p.i. day 12, and even at p.i day 14 their volume was several fold smaller than that of tumors generated by B16 wt cells. Size of tumors generated by silenced B16 cells in wt and P2X7R-KO mice is shown in Figure 9B, lower panel.

B16 cell were also stably transfected with a cytosolic luciferase (cytLuc) construct to allow tumor progression monitoring in the living animal by total body bioluminescence measurement (Figure 11). Interestingly, bioluminescence analysis allowed tumor detection in both mouse strains at least four days earlier than by calliper measurement, i.e. at p.i. day 5, vs p.i. day 9 (Figure 11D). Regrettably, bioluminescence analysis allowed reliable monitoring of tumor growth for only about 10-12 days, and up to a size of about 1000 mm^3. At later time points, photon emission declined and luminescence intensity did not any more correlate with the effective tumor size measured by calliper. At p.i. day 12, luminescence emission was similar in the KO and wt, as if tumors had reached a similar size in both mice strains.

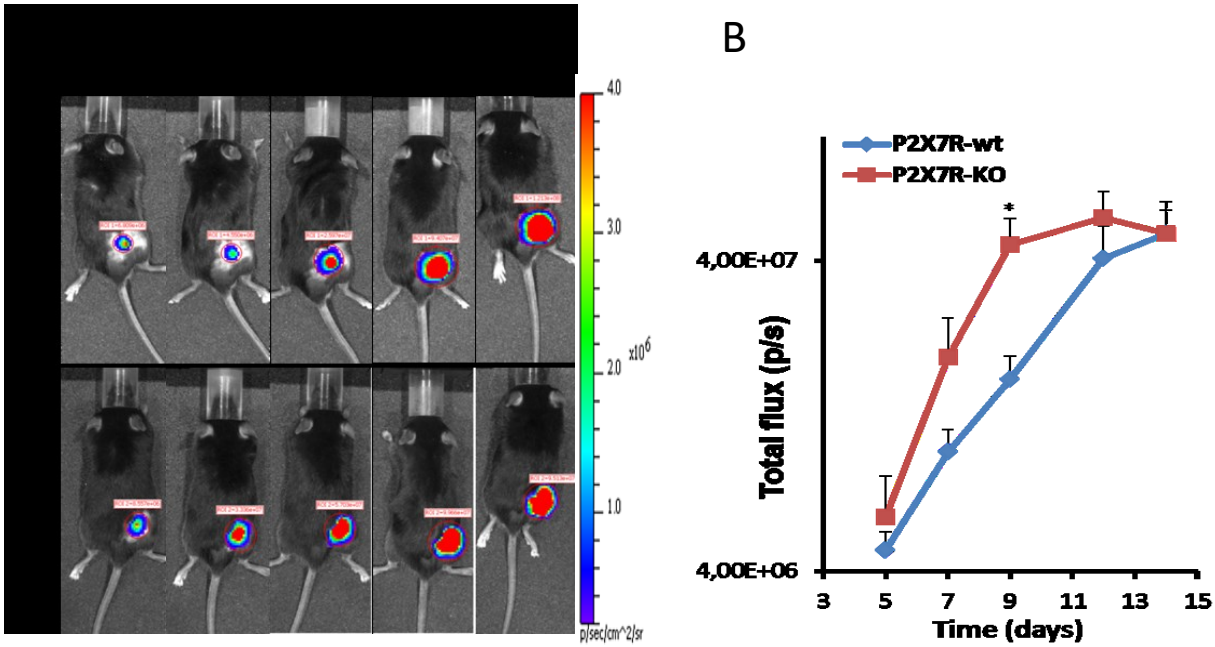

Figure 11. Subcutaneous B16 melanomas growth in P2X7R-wt and KO mice assessed at IVIS Lumina. **A** Representative time course of melanomas expansion in a P2X7R-wt and KO mice evaluated by luminescence recording. **B**, Kinetics of tumor growth in wt and P2X7R-KO mice estimated by cytLuc luminescence emission (photon/second, p/s) at the indicated post-injection days. Data are average ± SEM. *, $p < 0.05$.,

Lack of correlation between size estimated by luminescence and physical measurement by calliper was further confirmed by measurement of excised masses. *Post mortem* analysis showed that the apparent decrease in size of tumors growing in the P2X7R-KO host was due to massive intra-mass haemorrhagic necrosis that drastically reduced tumor cell number. Intra-mass necrosis decreased the number of light-emitting cells, thus artifactually decreasing luminescence emission, but had a comparatively smaller effect on whole tumor size (Figure 12).

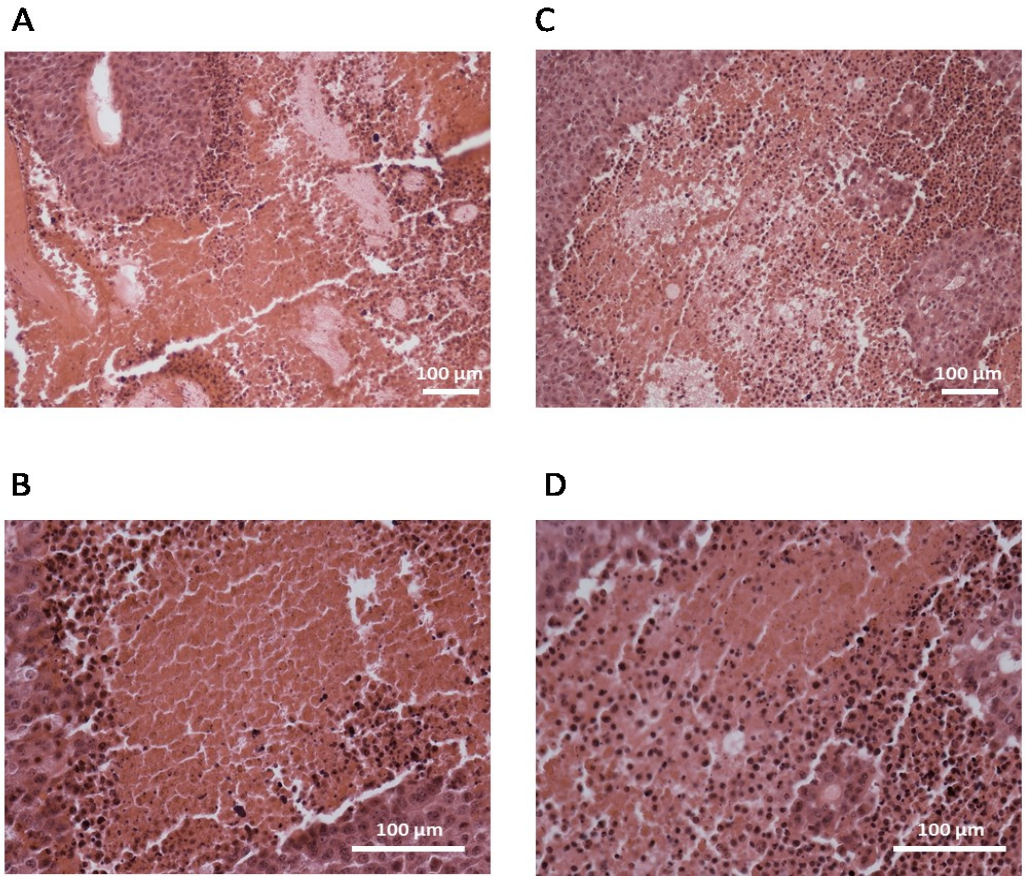

Figure 12. Core necrosis in B16 melanomas. Representative images of central necrosis of B16 melanoma masses in P2X7R-KO (A and B) or wt (C and D) mice. Specimens were fixed and stained with haematoxylin-eosin as described in Materials and Methods.

Colon carcinoma model

To explore the effect of P2X7R deletion in a mouse strain of a different genetic background hosting a tumor of a different histotype, we carried out similar experiments in BALB/cJ mice inoculated with the syngeneic CT26 murine colon carcinoma. Also in the BALB/cJ model deletion of the P2X7R caused a dramatic acceleration of tumor growth, especially at early time points (Figure 13A). After p.i. day 13, tumor growth slowed down, probably as a result of ensuing necrosis. *Ex-vivo* measurement of excised masses confirmed the results of the *in vivo* measurement (Figures 13B and 13C). Effect of P2X7R deletion on tumor growth was stronger in the BALB/c than in the C57Bl/6 mice. Up to p.i. day 13, the CT26 tumor (BALB/cJ host) was almost 5-6 fold larger in the P2X7R-KO than in the wt mice, while over the same time span the B16 tumor (C57Bl/6 host) was only 2-3 fold larger in the P2X7R-KO than in the wt. Of course, this could be due to the intrinsic biological features of the two tumors, but it might also depend on the different *p2x7R*

genetic variant expressed in the two mouse strains. In fact, C57Bl/6 mice are homozygous for an allelic loss-of-function mutation (P451L) that decreases P2X7R activity, while BALB/cJ mice carry the fully functional wt *p2x7R* alleles (P451) [127]. Thus, P2X7R-dependent responses in C57Bl/6-wt are about 50% weaker than those of BALB/cJ-wt, that is closer to the KO phenotype of both strains [122].

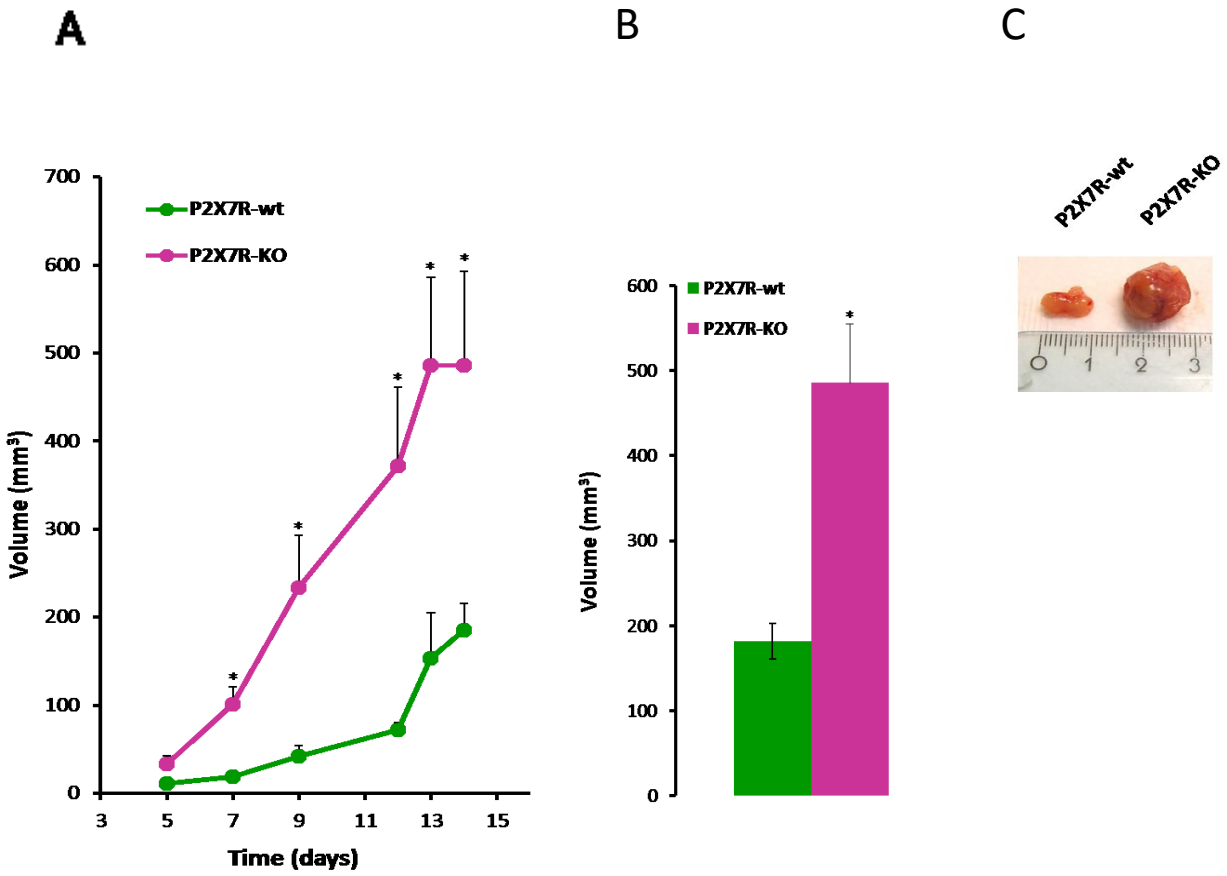

Figure 13. Accelerated growth of CT26 murine colon cancer in Balb/c P2X7-KO mice. **A**, Balb/c mice were subcutaneously inoculated into the right hind leg with CT26 cells ($2{,}5\times10^5$). Tumor volume was in vivo assessed by calliper measurement at the indicated time points. **B**, Volume of tumor masses after *post-mortem* excision. Data are averages ± SEM. * $p < 0.05$. **C**, Representative picture of tumor masses from P2X7R-wt (left) and P2X7R-KO mice (right).

Lung metastatic spreading of B16 melanoma is greater in P2X7R-KO than in wt mice

B16 melanoma is a widely used model for the study of metastatic dissemination, thus we set to investigate whether lack of host P2X7R might affect metastatic efficiency. Figures 14A and 14B show *in vivo* bioluminescence emission at p.i. day 18 from wt and P2X7-KO mice injected with B16 cells *via* the caudal vein. In 3 out of 6 of the P2X7-KO, but in none of the wt mice, luminescence emission from the thoracic cage was detectable at this time point. Figure 14C, reports a time course of luminescence emission from mice # 11 (wt) and # 4 (KO) showing that lung metastases were clearly detectable in the KO animal as early as p.i. day 15, but only at p.i. day 21 in the wt. By this time, luminescence emission in the KO mouse had already spread all over the thoracic cage. At p.i. day 21, mice were sacrificed and lungs examined for metastases. Figure 14D shows that number of metastatic foci in the lungs from the KO mouse was much higher than in the wt. Average lung metastases number from the two strains is shown in Figure 14E.

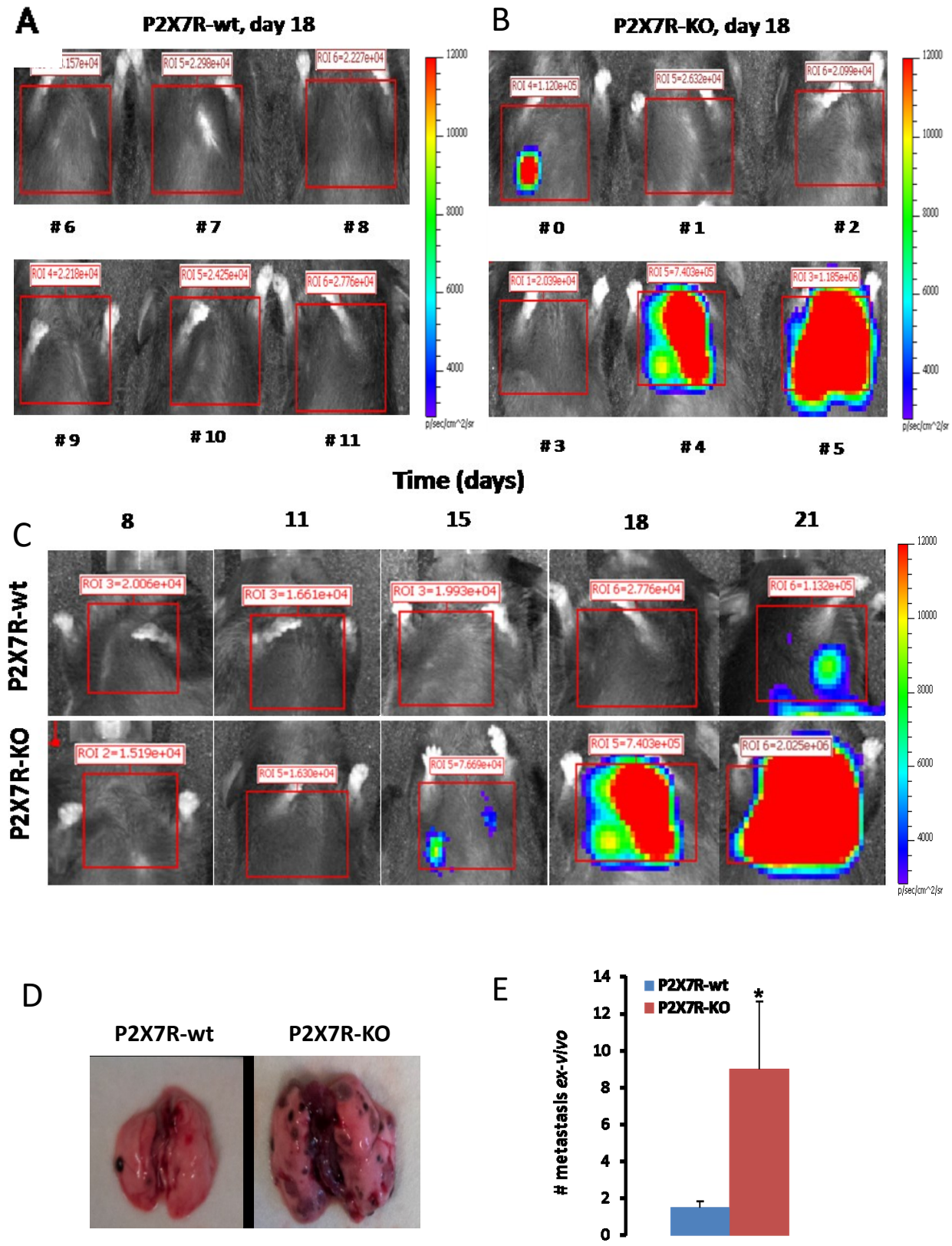

Figure 14. Dissemination of lung metastasis in wt and P2X7R mice assessed by luminescence emission. Six wt (**A**) and P2X7R-KO (**B**) mice at post-injection d 18 are shown. Numbers below panels indicate mouse number. **C**, Kinetics of lung metastasis dissemination assessed by luminescence recording at the indicated post-injection days. **D**, Picture of lungs from wt and P2X7R mice shown in panel C and sacrificed at p.i. d 21. **E**, average ± SEM lung metastases number in wt and P2X7R-KO mice. * $p < 0.05$

Reduced inflammatory infiltrate in primary B16 melanoma and B16 melanoma lung metastasis in P2X7R-KO versus P2X7R-wt mice

Infiltration by inflammatory cells is a feature of malignant tumors that can be helpful or detrimental for the host, depending on whether the inflammatory infiltrate supports an anti-tumor immune response or immunosuppression. To our surprise, histology of B16 tumors from P2X7-KO mice showed very little if any inflammatory infiltrate, whether at the tumor/connective tissue interface or within the tumor mass (Figures 15A-C). On the contrary, tumors growing in wt mice showed, as expected, a massive inflammatory cell infiltrate in the peritumoral connective tissue (Figure 15D), at the tumor/connective tissue interface (Figure 15E) and within the tumor itself (Figure 15F).

As a further proof of the absence of inflammatory cell infiltration, tumors were stained with anti-CD3 and anti-F4/80 Abs to highlight the presence of T lymphocytes and macrophages/DCs. As shown in Figures 16A and 16C, few if any T lymphocytes or mononuclear phagocytes were identified in specimens from the KO mice. See for comparison specimens from wt mice (Figures 16B and 16D). The tumor-infiltrating T lymphocyte population in the P2X7R-wt host was largely made by $CD8^+$ cells, as shown by specific staining in Fig. 16E and 16F.

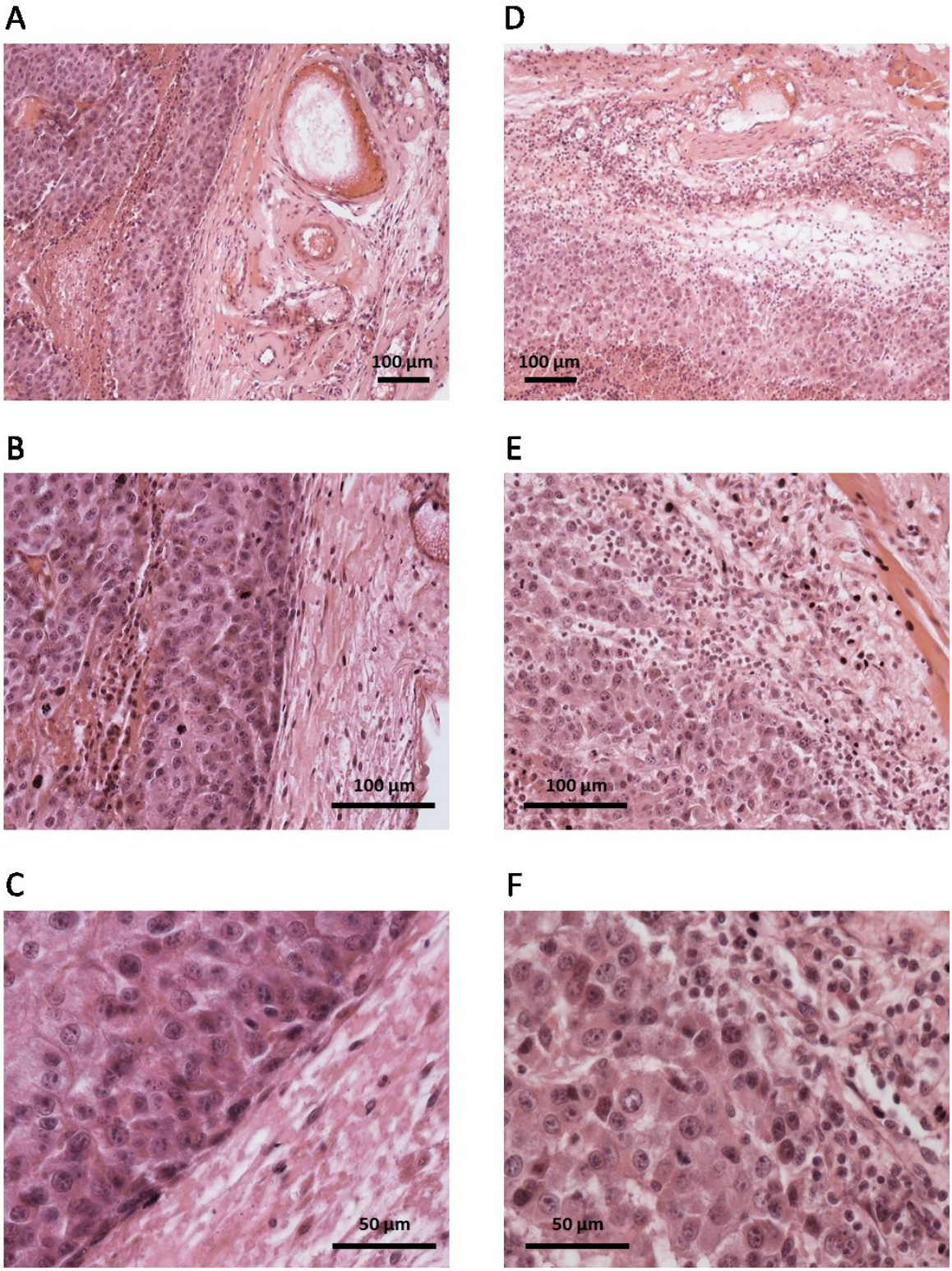

Figure 15. Lack of inflammatory infiltrate in B16 melanomas primary tumors grown in P2X7R-KO mouse. Specimens from P2X7R-KO (**A**–**C**) or wt (**D**–**F**) mice were stained with H&E as described in Materials and Methods. 10×, 20×, 40× magnification are shown from top to bottom.

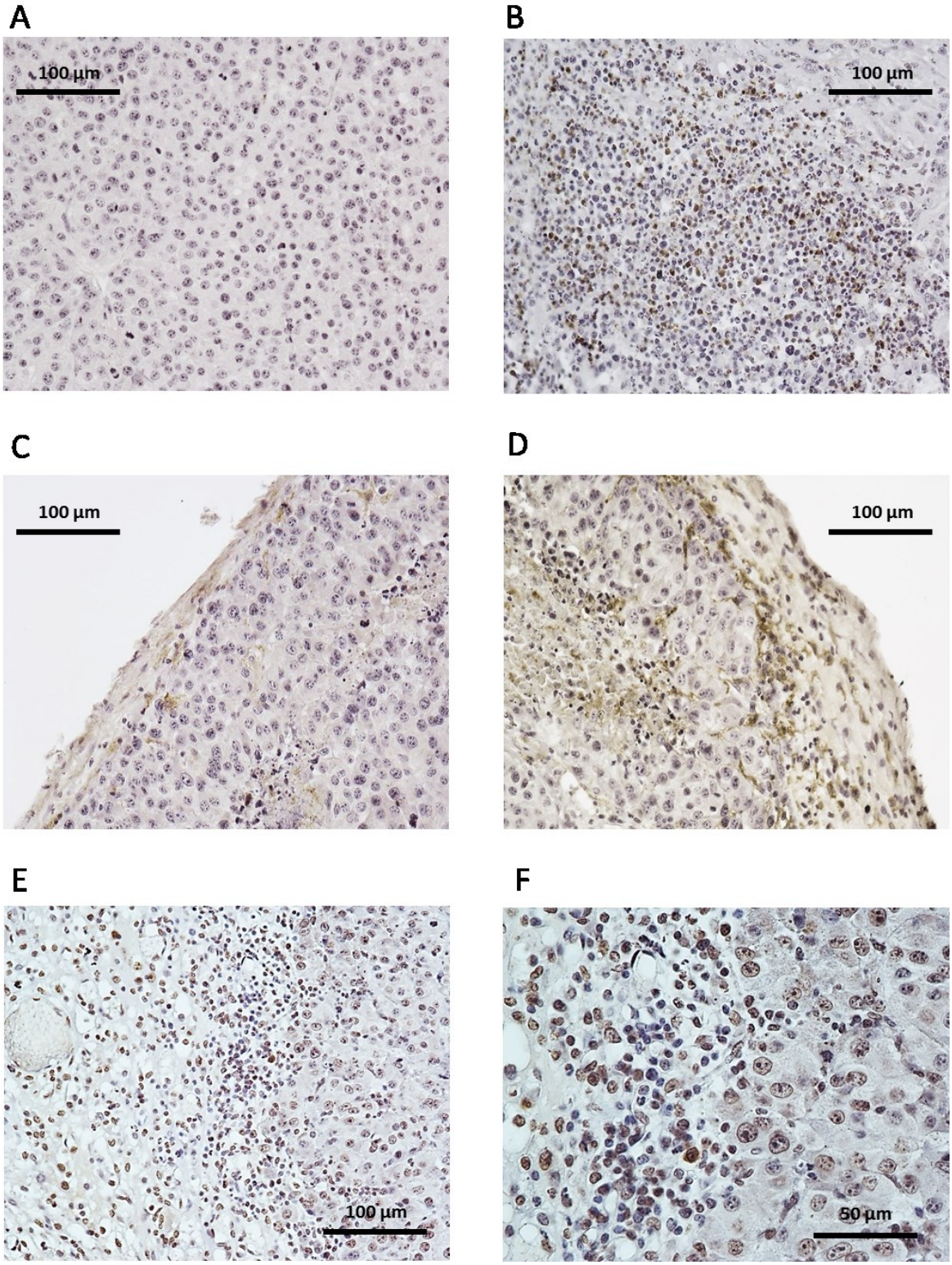

Figure 16. B16 melanomas growing in the P2X7R-KO host lack T lymphocyte and macrophage infiltrate.**A** and **B**, primary B16 tumor from P2X7R-KO or wt mice, respectively, stained with anti-CD3 Ab (20× magnification). **C** and **D**, primary B16 tumor from P2X7R-KO or wt mice, respectively, stained with anti-F4/80 mAb (20× magnification). **E** and **F**, B16 primary tumor from P2X7R-wt host stained with anti-CD8 mAb. Samples were stained with H&E as described in Materials and Methods. E 20× magnification, F 40× magnification.

As in the primary subcutaneous tumor, lung metastases in the KO animal showed virtually no inflammatory cell infiltrate, whether in the tumor mass or at the tumor/healthy tissue interface. Furthermore, the distal lung tissue showed no signs of an inflammatory reaction, i.e. thickening of alveolar septa or increased number of alveolar macrophages (Figures 17A and 17B). On the contrary, lungs from wt mice showed diffuse signs of inflammation, both in the peritumoral and in the distal lung tissue (Figures 17D and 17E).

CD3 immunostaining showed T lymphocyte infiltration in the metastases from the wt but not from the KO mouse (Figures 17C and 5F).

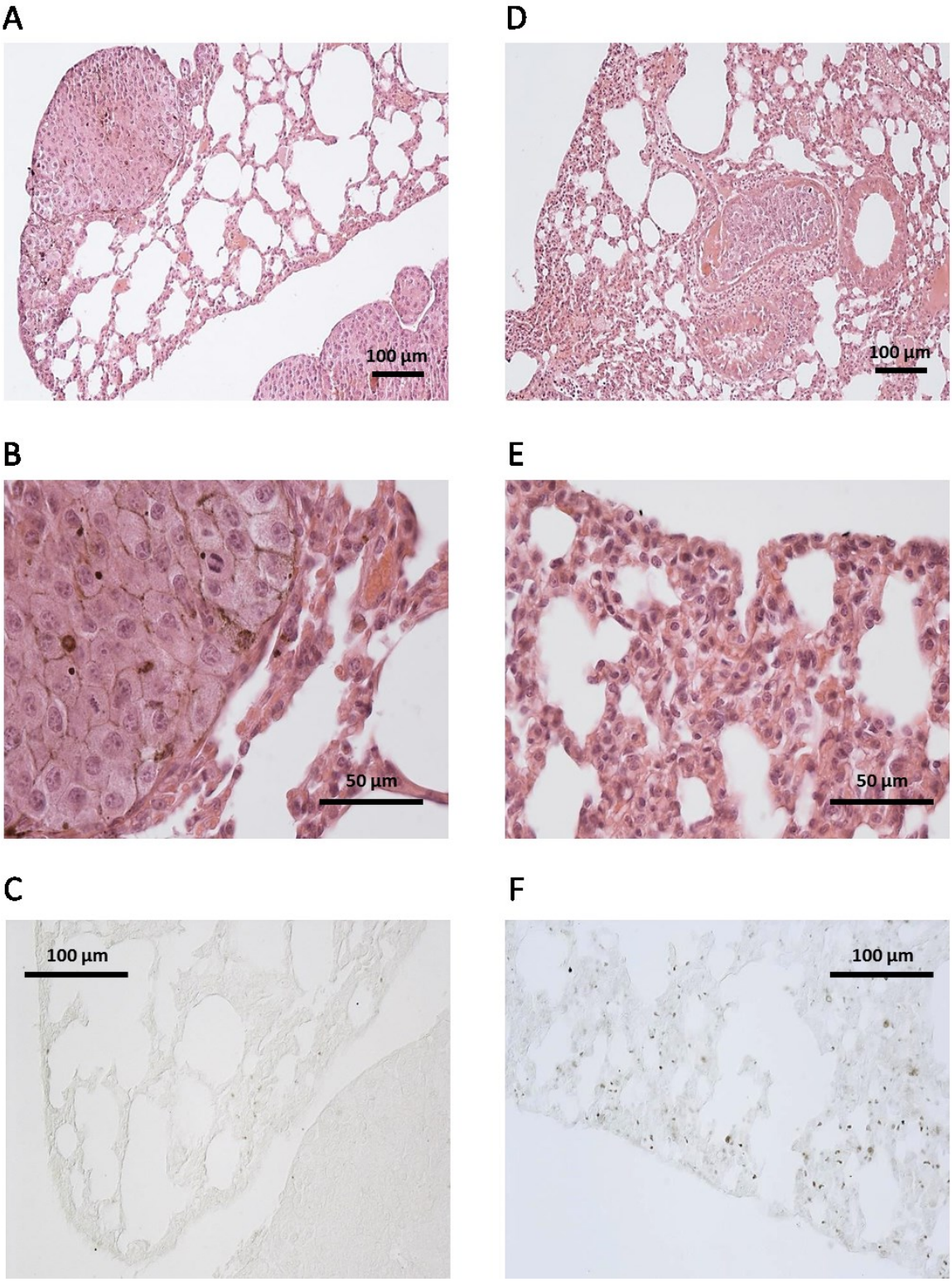

Figure 17. Lung metastases of B16 melanoma from P2X7R-KO mice lack inflammatory cell infiltration. Specimens from P2X7R-KO (**A**-**C**) or wt mice (**D**–**F**). Specimens A, B, D, and E were fixed and stained with H/E, whereas specimens C and F were stained with anti-CD3 Ab without hematoxylin counterstaining. A and D 10× magnification, B and E 40× magnification, C and F 20× magnification.

P2X7R deletion on immune cells causes accelerated growth in P2X7R-wt mice reconstituted with P2X7R-KO bone marrow.

Absence of inflammatory infiltrate suggested that accelerated tumor growth in the P2X7R-KO host might be due to inefficient immune response. Thus, we investigated the effect of selective P2X7R deletion on hematopoietic cells by generating BALB/cJ P2X7R chimeric mice. Chimeras were obtained by inoculating P2X7R-KO bone marrow into P2X7R-wt recipient mice (P2X7R-KO>P2X7R-wt chimeras), or on the contrary P2X7R-wt bone-marrow into P2X7R-KO mice (P2X7R-wt>P2X7R-KO chimeras). We also reconstituted P2X7R-KO recipients with P2X7R-KO bone marrow (P2X7R-KO>P2X7R-KO mice) and P2X7R-wt recipients with P2X7R-wt bone marrow (P2X7R-wt>P2X7R-wt) as controls. As shown in Figure 18, tumor proliferated to a higher rate in P2X7R-KO>P2X7R-wt than in P2X7R-wt>P2X7R-wt or P2X7R-wt>P2X7R-KO chimeras, indicating that lack of P2X7R expression on immune cells was a main cause for the accelerated growth observed in the P2X7R deleted host.

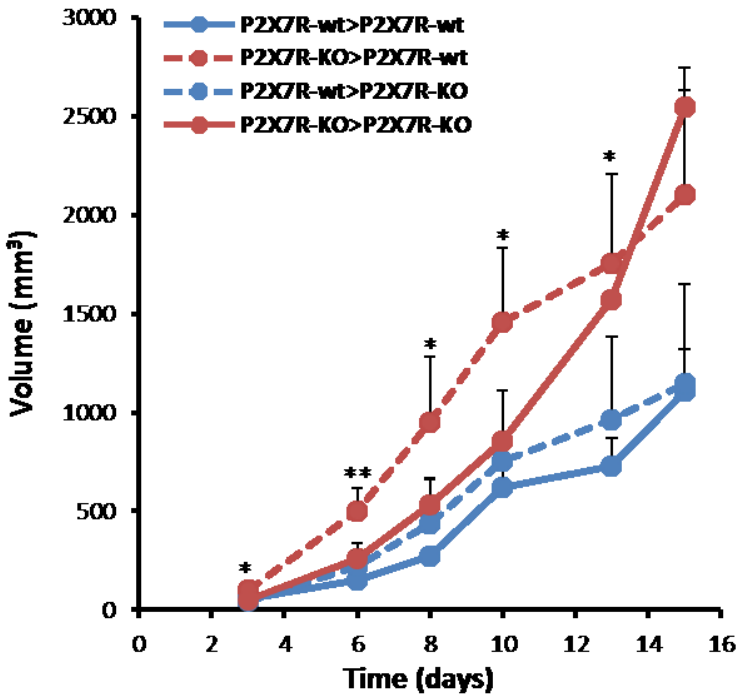

Figure 18. Analysis of tumor growth in P2X7R-KO>P2X7R-wt chimeras. Tumor growth in P2X7R-wt>P2X7R-KO, P2X7RKO>P2X7R-wt, P2X7R-KO>P2X7R-KO, and P2X7R-wt>P2X7R-wt chimeric mice. BMT was performed as described in Materials and Methods. Data are average ± SEM. (n=4). *, $p < 0.05$; **, $p < 0.01$ for P2X7R-KO>P2X7R-wt versus P2X7R-wt>P2X7R-wt, by one-tail unpaired t test.

IL-1β cytokine content in P2X7R-wt and KO mice bearing B16 melanomas.

One of the main responses triggered by P2X7R stimulation is IL-1β release. This cytokine has a pivotal role in inflammation and host-tumor interactions and drives intra-tumor inflammatory cell recruitment. An increase in IL-1β plasma levels is considered a poor prognostic factor in melanoma [128, 129]. Figure 20A, shows that blood IL-1β levels in tumor-bearing wt mice were about twice as high as in P2X7R-KO mice. A drastic decrease in IL-1β serum levels was anticipated in the P2X7R-KO mice as previous *in vitro* as well as *in vivo* experiments show that this receptor is a near absolute requirement for IL-1β release evoked by different stimuli such as extracellular nucleotides, LPS, anti-collagen Abs, or C3a [130-133]. Nevertheless, since it is well known that melanomas are a source of IL-1β [129], it was not surprising that P2X7R deletion did not entirely suppress serum levels of this cytokine. Next, we analyzed IL-1β content of excised tumor masses. As shown in Figure 20B, excised tumor masses from KO mice contained IL-1β, although to an at least four-fold lower amount compared to melanomas from wt animals. To highlight the contribution of melanoma cells to IL-1β release, we also measured IL-1β content of tumors generated by P2X7R-silenced B16 cells, which was markedly reduced in the wt and nearly abolished in the KO host (Figure 20B).

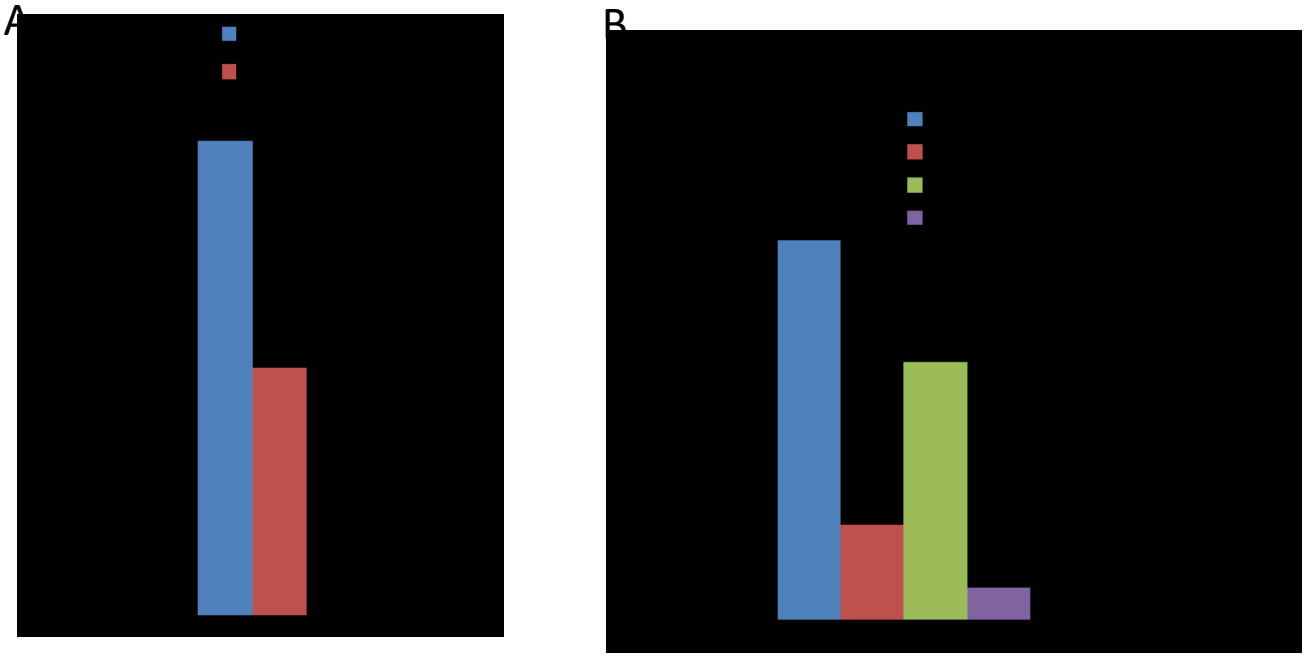

Figure 20. Interleukin-1β release in wt and P2X7R-KO mice. **A** Intereleukin-1β plasma levels. **B** Intra mass IL-1β content.

Reduced intra-mass IL-1β content suggested that lack of P2X7R impaired tumor interaction with host immune cells. To test this hypothesis, DCs were isolated from mouse bone marrow and challenged with B16 cells. As shown in Figure 21, challenge of DCs from wt mice triggered a large IL-1β release, that was reduced to about one third in DCs from P2X7R-KO mice.

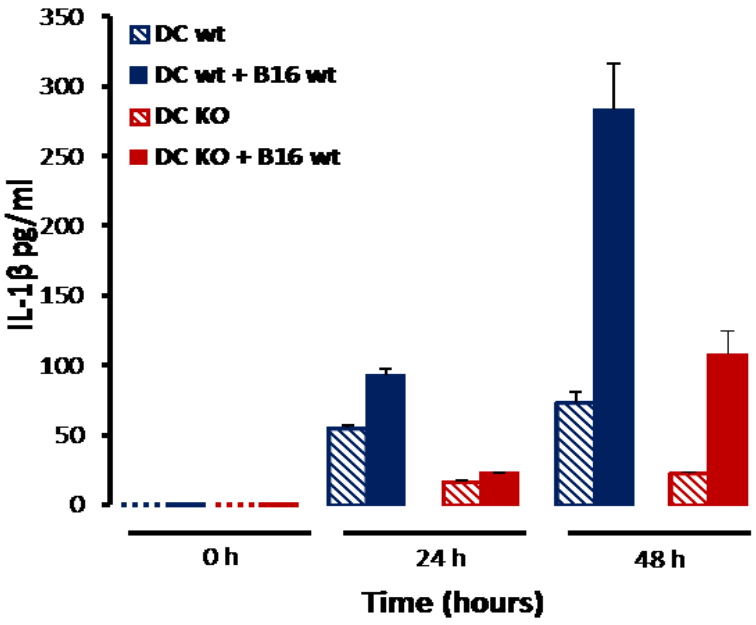

Figure 21. IL-1β content of supernatant of B16 wt and either P2X7R-wt or P2X7R-KO DCs co-cultures.

VEGF cytokine content in P2X7R-wt and KO mice bearing B16 melanomas.

In a recent study we showed that secretion of the key angiogenic factor VEGF is critically dependent on P2X7R [88], thus we checked if release of this growth factor was reduced in P2X7R-KO mice. As shown in Figure 22A, B16 melanoma cells *in vitro* release VEGF in a P2X7R-dependent fashion. P2X7R dependency was confirmed by *ex vivo* measurements showing that melanoma tumors from P2X7R-KO animals released a VEGF amount that was about 50% of that secreted by tumors from wt mice (Figure 22B). Tumor VEGF content was further reduced in tumors generated by P2X7R-silenced B16 cells in P2X7R wt mice, and almost completely obliterated in silenced B16 tumors grown in P2X7R-KO mice (Figure 7B). This experiment gives two valuable information: a) the near totality of *in vivo* VEGF release is dependent on P2X7R; b) although reduced, VEGF release in the P2X7R-KO host is sufficient to support fast tumor growth. *In situ* VEGF release was confirmed by staining excised tumor masses with an anti-VEGF mAb. In agreement with

the ELISA assay, immunohistochemistry showed a lower content of VEGF in tumors from P2X7R-KO mice (Figures 22C-F).

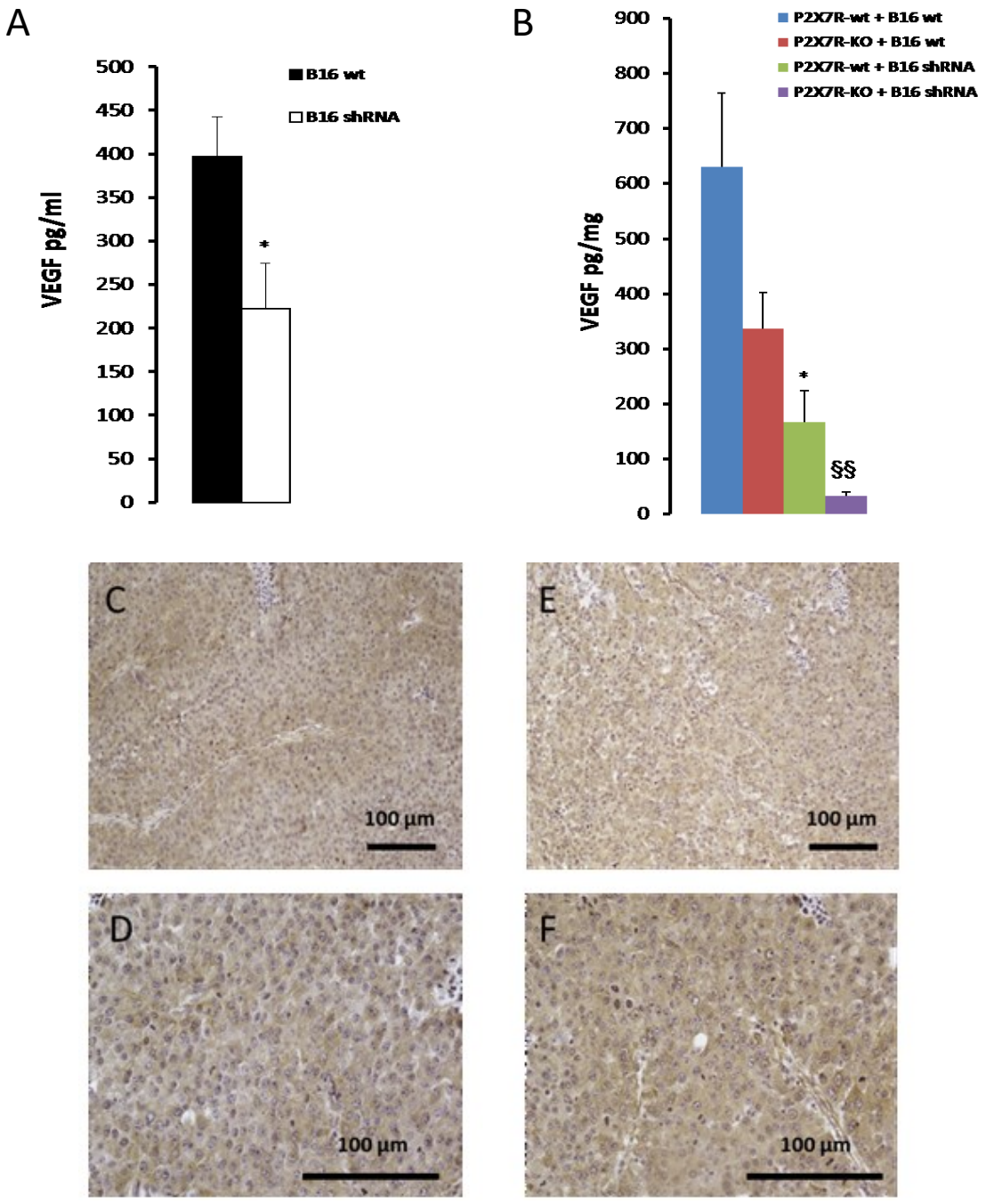

Figure 22. Effect of P2X7R deletion on VEGF release. **A**, in vitro VEGF release from wt or P2X7R-silenced B16 cells. **B**, intra-tumor VEGF content of B16-wt or P2X7R-silenced tumors grown in wt or P2X7R-KO mice. VEGF was measured by ELISA. A, * $p < 0.05$ for B16 shRNA vs B16-wt. B, * $p < 0.05$ for P2X7R-wt + B16 shRNA vs P2X7R-wt + B16-wt; ** $p < 0.01$ for P2X7R-KO + B16 shRNA vs P2X7R-KO + B16-wt. **C-F**, VEGF staining of tumors from P2X7R-KO (C and D) or wt (E and F) mice. Specimens were fixed and stained with the anti-VEGF Ab as described in Materials and Methods.

P2X7R deletion impairs N13 cell migration ability

Lower intra-tumor IL-1β levels might explain a reduced inflammatory infiltrate, however the lack of inflammatory response found in the P2X7R-KO mice was so striking that we hypothesized that P2X7R deletion caused a more profound, basic, defect in immune cell migration. Thus, we performed a simple *in vitro* wound healing experiment by using N13 mouse microglial cells. N13 cells have been widely used to study P2X7R responses, and from this cell line we selected several clones lacking P2X7R [109]. One of such clones, N13R, was used in the experiments shown in Figure 23A-F. N13-wt and N13R cells were layered in a cell culture dish and, after reaching confluence, the monolayer was wounded with a pipette tip. N13-wt microglia cells migrated from both sides of the wound and within 12 hours re-established the continuity of the monolayer. On the contrary, N13R cells were utterly unable to repopulate the wound. In particular, live recording showed that N13R cells were motile, but apparently incapable of directional migration. This experiment suggested that lack of P2X7R hinders the basic ability of inflammatory cells to progress along a chemotactic gradient, and thus infiltrate the tumor.

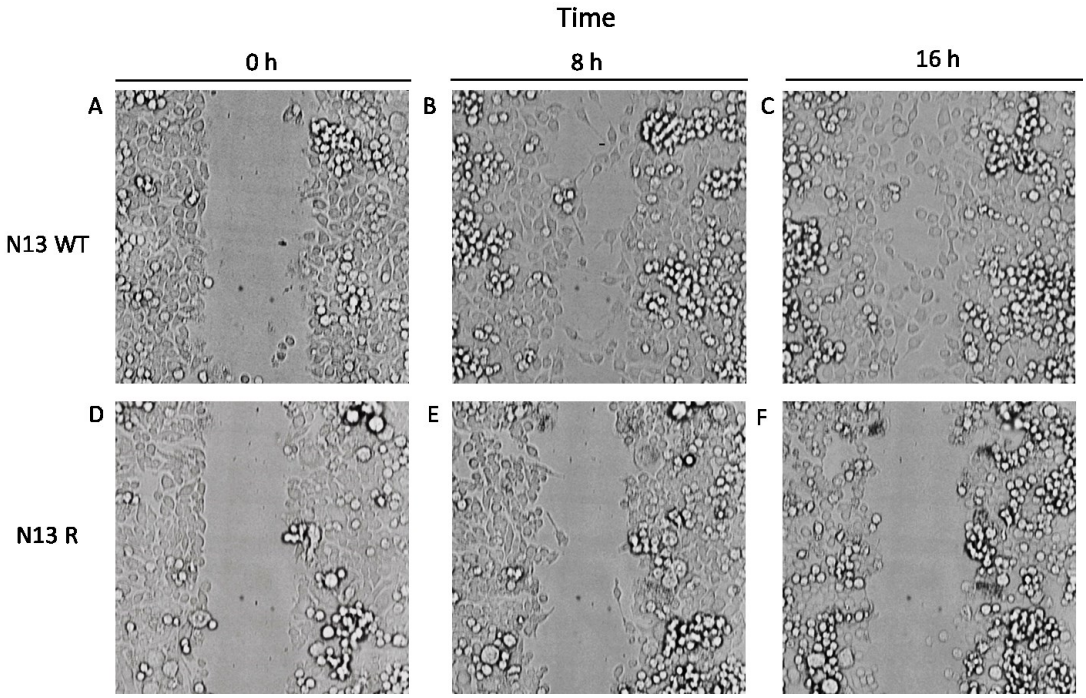

Figure 23. P2X7-less N13 mouse microglia cells have impaired wound-healing ability. N13 and N13R cells were seeded in Petri dishes and allowed to reach confluence before scratching. At this point, the monolayer was scratched with a pipette tip and cell migration recorded for 16 hours.

Systemic administration of P2X7R blockers reduced B16 melanomas growth

In our previous work we showed that pharmacological P2X7R blockade or silencing have a strong anti-tumor effect in both the *nude/nude* and syngeneic immunocompetent host [88]. In these experiments the P2X7R blockers were administered directly into the tumor mass, thus maximizing blockade of tumor rather than host P2X7R. It might be objected that this administration route might have masked possible untoward effects of P2X7R antagonism on host P2X7R, and being unpractical in humans, would be of little help in view of possible applications to anti-cancer therapy. To tackle this objection, two highly selective P2X7R blockers were intra-peritoneally (i.p.) administered to P2X7R-wt tumor bearing mice. As shown in Figure 24, both blockers had a strong inhibitory effect on tumor growth compared to vehicle-injected mice, thus showing that P2X7R blockers have a strong anti-cancer activity, even when systemically administered.

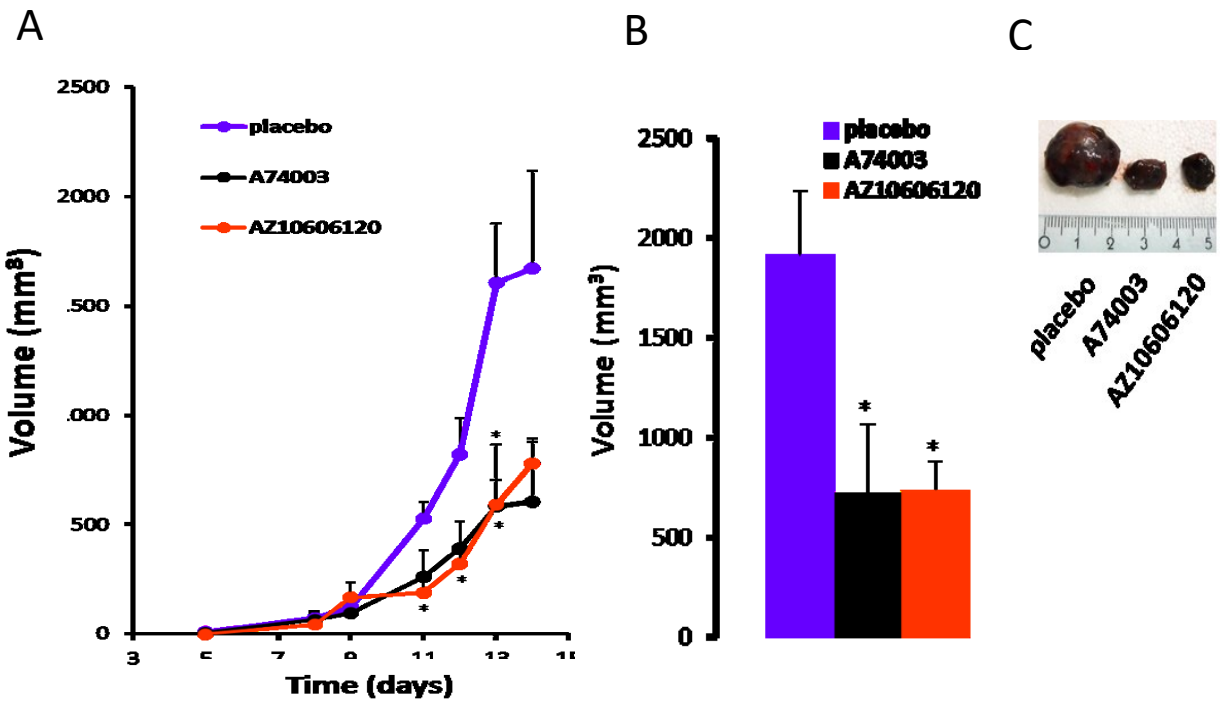

Figure 24. Effect of i.p. administration of P2X7R blockers on tumor growth in the P2X7R-wt host. Mice were inoculated with B16 cells (5×10^5) as described in Fig. 1 and, starting at day 5, i.p. injected every 2 days with 100 µl of A74003 (10 mmol/L), AZ10606120 (300 nmol/L), or placebo. **A**, *in vivo* kinetics of tumor growth. **B**, tumor size after *postmortem* excision. **C**, representative picture of tumor masses from placebo and P2X7R antagonist-injected mice. Data are average ± SEM (n=5). *, $p < 0.05$ versus placebo.

DISCUSSION

Increasing evidence shows that the tumor microenvironment plays a key role in moulding the anti-cancer host immune response [134]. This is due to the peculiar immunosuppressive and pro-angiogenic properties of this restricted milieu, thus anti-tumor therapeutic strategy must by necessity tackle an adverse environment. Over recent years the immunological and biochemical properties of tumor interstitium have been explored in great detail, thus allowing the design of innovative approaches to cancer therapy. The tumor microenvironment is heavily infiltrated by inflammatory cells, and rich in immunosuppressive and angiogenic factors such as IL-10, TGF-β, adenosine, arginase, VEGF and FGF [135, 136]. Furthermore, we have recently shown that the tumor interstitium is also rich in extracellular ATP [18, 121]. Extracellular ATP is attracting increasing interest because it is now well established that this nucleotide, besides its undisputed role in intracellular energy transactions, has a key extracellular messenger role [137]. Under physiological conditions, and in healthy tissues, the extracellular ATP concentration is in the nanomolar range [138], however, as a consequence of tissue damage or inflammation, extracellular ATP may rise to the high micromolar level and up to hundred micromolar in the microenvironment of different tumors [18, 121, 139]. These findings raise the question of the pathophysiological significance of an elevated tissue interstitium ATP content in host-tumor interactions. Extracellular ATP is a pleiotropic agonist, it is therefore likely that it might modulate host-tumor interaction in different ways: as a chemotactic factor for inflammatory cell migration, a stimulus for pro-inflammatory cytokine release, a trophic agent supporting tumor cell proliferation, and a source of additional immunomodulatory agents such as adenosine.

Expression by host and tumor cells of different P2YRs and P2XRs with widely different affinity confers to purinergic signalling an astonishing plasticity. However, most P2R subtypes have high affinity for extracellular nucleotides, suggesting that at the elevated ATP concentrations found within the tumor microenvironment they must be fully desensitized. This is not the case for at least one P2 receptor, P2X7R, thanks to its low affinity for ATP and its non-desensitizing behaviour [10, 40]. ATP acts on P2X7R with an EC_{50} in the 100-300 μM range, a feature that might even raise the question of whether this receptor is ever active under physiological conditions; but in the tumor-associated ATP-rich milieu the P2X7R might well find the appropriate conditions for activation.

P2X7R is currently considered a pro-inflammatory receptor in view of its ability to cause a massive secretion of mature IL-1β and other cytokines of the IL-1 family, stimulate ROS generation, cause metalloprotease release and trigger intracellular pathogen killing [101, 140, 141]. In addition, overstimulation with high ATP doses or with the pharmacological ATP analogue BzATP cause cell death by necrosis or apoptosis [142, 143]. Interestingly, several reports now show that under conditions of tonic stimulation by endogenously-released ATP, i.e. in the absence of stimulation with pharmacological ATP doses, P2X7R may also act as a growth-promoting receptor [47, 83, 88]. Thus, it is to be expected that P2X7R should be active on both the tumor and the host cells, with a final outcome difficult to anticipate.

Most tumors express P2X7R to high level, and are dependent on its function for growth and metastatization [22, 144]. The powerful growth-promoting activity of P2X7R is mediated by an array of metabolic changes that have been dissected in detail in our laboratory [83, 85, 90]. In tumor cells, P2X7R is constantly and tonically active, thus causing: a) moderate increase in the endoplasmic reticulum and mitochondrial Ca^{2+} concentration, b) enhanced efficiency of oxidative phosphorylation; c) an increase in intracellular ATP stores, d) activation of the transcription factor NFATc1, e) stimulation of aerobic glycolysis, and f) higher proliferation rate [48, 83]. These *in vitro* metabolic changes have striking *in vivo* correlates, as we and others have shown that P2X7R silencing or pharmacological blockade strongly reduce, while P2X7R overexpression accelerates, tumor growth [88, 93].

In the present study we investigated the role played by host P2X7R in anti-tumor response. By using P2X7R-KO mice of two different strains we show that expression of a functional P2X7R by host immune cells is an absolute requirement for an efficient anti-tumor response. B16 melanoma cells proliferated to a rate two-fold faster in the *p2x7R*$^{-/-}$ than in the wt C57Bl/6 host, and number of lung metastases was about four times larger in KO than in wt mice. In the P2X7R-KO BALB/cJ strain, growth rate was even faster compared to the wt, especially during the initial phase of growth. This latter finding further highlights the fundamental contribution of P2X7R to the control of tumor growth since the C57Bl/6 strain is homozygous for a loss-of-function mutation that causes a P415L substitution that encodes a hypofunctional form of the P2X7R [127]. This puts C57Bl/6 mice somewhat halfway between a P2X7R-wt and a P2X7R-KO strain. On the contrary, the BALB/cJ strain carries the fully functional wt P2X7R, thus phenotypic differences with the KO are more clear cut.

A main cause for the inability of *p2x7R*$^{-/-}$ hosts to control tumor progression is likely to be the patent lack of an anti-tumor immune response. The crucial role of P2X7R expression on host hematopoietic cells in antitumor response was further confirmed by generating P2X7R chimeric mice. P2X7R-KO>P2X7Rwt chimeras allowed a much faster tumor growth than P2X7Rwt>P2X7R-KO chimeras, thus closely replicating tumor growth kinetics observed in the P2X7R-KO host. Accordingly, P2X7RKO>P2X7R-KO mice allowed a faster tumor growth thanP2X7R-wt>P2X7R-wt mice. Although in the P2X7R-wt host the tumor was heavily infiltrated by $CD8^+$ lymphocytes and mononuclear phagocytes, in the P2X7R-KO host both the primary tumor and the metastatic sites showed virtually no inflammatory cell infiltrate. Thus, we were unable to characterize infiltrating immune cells in the specimens from the P2X7R-KO mice.

Intra-mass levels of IL-1β and VEGF, two factors known to be released in response to P2X7R stimulation [72, 88, 145], were accordingly much lower in tumors growing in *p2x7R*$^{-/-}$ than in wt mice. Interestingly, while blood IL-1β was low in the KO host, as expected on the basis of the known phenotype of the P2X7R-KO mouse, intra-mass levels of this cytokine were elevated, although not to the same level as in the wt host. This discrepancy between intra-tumor and peripheral IL-1β levels is due to intrinsic IL-1β-releasing activity of the B16 melanoma [129]. Inability of immune cells from P2X7R-deleted host to release IL-1β was clearly confirmed by direct *in vitro* stimulation of bone marrow-derived DCs with B16 melanoma cells. Lack or response of immune cells from P2X7R-KO mice to stimulation with tumor cells is in keeping with previous results showing that mouse DCs lacking P2X7R fail to secrete IL-1β and to stimulate Ag-specific T_H lymphocytes [109].

Impairment of inflammatory cell recruitment may also be due to an intrinsic defect in chemotaxis of P2X7R-deleted immune cells. Our *in vitro* data show that cells deleted of P2X7R have a reduced ability to migrate in a typical *in vitro* wound repair model, suggesting that lack of P2X7R hinders cell chemotaxis ability and thus tumor infiltration. The P2X7R itself, at variance with other P2 receptors, is not currently considered a chemotactic receptor but rather a membrane pathway that, by allowing ATP release, enhances the ATP-based chemotactic gradient [143, 146]. An efficient ATP-based chemotaxis requires a controlled nucleotide release at the leading edge of the chemotacting cell [146], a process that might be highly inefficient in the absence of P2X7R.

Previous findings by our laboratory showed that P2X7R blockade by oxidized ATP or PPADS did not prevent macrophage chemotaxis in response to non-nucleotide chemotactic

factors [147], thus supporting the view that P2X7R has a main role as a pathway for ATP efflux rather than as true chemotactic receptor. Lack of inflammatory cell infiltration in the P2X7R-deleted host has also been recently observed in model of chronic skin inflammation [148].

Inability of immune cells from P2X7R-KO mice to respond to stimulation by tumor cells is in keeping with previous results from our laboratory showing that mouse DCs lacking P2X7R failed to secrete IL-1β and to stimulate Ag-specific T_H lymphocytes [109]. Interestingly, in the experiments by Mutini et al. Ag-presenting activity was fully restored by supplementation of exogenous IL-1β [109]. Similar results were more recently obtained by Zitvogel and co-workers [110]. Altogether, low IL-1β levels in the tumor-bearing P2X7R-KO mice, lack of IL-1β-releasing activity in B16-challenged P2X7R-KO DCs, and deficient chemotaxis of P2X7R-deleted immune cells suggest an intrinsic deficit to respond to tumor cell stimulation.

Release of VEGF into the tumor interstitium is a potent stimulus for tumor progression by promoting angiogenesis and cancer stem cell survival and differentiation [149]. We have shown that in human and mouse tumors *in vivo* VEGF is secreted in a P2X7R-depedent fashion and gives an essential contribution to tumor growth [88]. Present data suggest that contribution of VEGF to melanoma growth in the *p2x7R*$^{-/-}$ host is less important than in other tumor models, since VEGF levels in the P2X7R-KO mice were reduced to about 50% of those measured in the wt, and yet in the KOs tumor growth was much faster. Both host and tumor cells contributed to VEGF secretion, as it was possible to abrogate VEGF release in vivo only by ablating P2X7R function both in the host (P2X7R-KO) and in the tumor (P2X7R silencing).

Given the key role of host P2X7R in the anti-tumor immune responses, highlighted in the present study, use of P2X7R blockers as anti-cancer therapy might appear problematic. We previously showed that intra-mass injection of P2X7R inhibitors is an effective anti-tumor treatment [88]. However, it might be objected that by injecting P2X7R blockers directly into the tumor, a route that is not usually amenable in humans, we maximized inhibition of the tumor P2X7R, and minimized possible inhibitory effects on the host immune cell P2X7R. Untoward inhibitory effects on host P2X7R might on the contrary be more relevant if the systemic administration route is followed. In the present study we provide a definitive answer to this criticism by showing that i.p. (systemic) administration of P2X7R antagonists was as effective as intra-mass injection. Thus, also in the case of systemic administration of P2X7R blockers, the tumor growth-inhibitory effect prevails on the

inhibition of host immune response. Since P2X7R blockade has an immunodepressive activity, like many anticancer agents currently used (e.g. rapamycin), it appears conceivable that a mild immunodepressive effect is the price to be paid to achieve anti-cancer activity.

Finally, our study shows that in an animal model genetically deleted of a receptor implicated in innate immunity tumor growth and metastatic spreading progress unimpeded, thus highlighting the complex role of inflammation in host-tumor interaction.

In conclusion, we have identified P2X7R as a non redundant host factor in *in vivo* anticancer response.

REFERENCES

1. Knowles, J.R., *Enzyme-catalyzed phosphoryl transfer reactions.* Annu Rev Biochem, 1980. **49**: p. 877-919.
2. Lohmann, K., *Über die pyrophosphatfraktion im muskel.* Naturwissenschaften, 1929. **17**(31): p. 624-625.
3. Drury, A. and A.v. Szent-Györgyi, *The physiological activity of adenine compounds with especial reference to their action upon the mammalian heart.* The Journal of physiology, 1929. **68**(3): p. 213.
4. Lazarowski, E.R., R.C. Boucher, and T.K. Harden, *Constitutive release of ATP and evidence for major contribution of ecto-nucleotide pyrophosphatase and nucleoside diphosphokinase to extracellular nucleotide concentrations.* Journal of Biological Chemistry, 2000. **275**(40): p. 31061-31068.
5. Di Virgilio, F. and M. Vuerich, *Purinergic signaling in the immune system.* Auton Neurosci, 2015. **191**: p. 117-23.
6. Yegutkin, G.G., *Enzymes involved in metabolism of extracellular nucleotides and nucleosides: functional implications and measurement of activities.* Crit Rev Biochem Mol Biol, 2014. **49**(6): p. 473-97.
7. Verkhratsky, A. and G. Burnstock, *Biology of purinergic signalling: its ancient evolutionary roots, its omnipresence and its multiple functional significance.* Bioessays, 2014. **36**(7): p. 697-705.
8. Hilton, S.M. and P. Holton, *Antidromic vasodilatation and blood flow in the rabbit's ear.* J Physiol, 1954. **125**(1): p. 138-47.
9. Burnstock, G., D.G. Satchell, and A. Smythe, *A comparison of the excitatory and inhibitory effects of non-adrenergic, non-cholinergic nerve stimulation and exogenously applied ATP on a variety of smooth muscle preparations from different vertebrate species.* Br J Pharmacol, 1972. **46**(2): p. 234-42.
10. Ralevic, V. and G. Burnstock, *Receptors for purines and pyrimidines.* Pharmacol Rev, 1998. **50**(3): p. 413-92.
11. Burnstock, G., *Pathophysiology and therapeutic potential of purinergic signaling.* Pharmacol Rev, 2006. **58**(1): p. 58-86.
12. Ferrari, D., et al., *The P2 purinergic receptors of human dendritic cells: identification and coupling to cytokine release.* FASEB J, 2000. **14**(15): p. 2466-76.
13. Bours, M.J., et al., *Adenosine 5'-triphosphate and adenosine as endogenous signaling molecules in immunity and inflammation.* Pharmacol Ther, 2006. **112**(2): p. 358-404.
14. Placido, R., et al., *P2X(7) purinergic receptors and extracellular ATP mediate apoptosis of human monocytes/macrophages infected with Mycobacterium tuberculosis reducing the intracellular bacterial viability.* Cell Immunol, 2006. **244**(1): p. 10-8.
15. Idzko, M., D. Ferrari, and H.K. Eltzschig, *Nucleotide signalling during inflammation.* Nature, 2014. **509**(7500): p. 310-7.
16. Roger, S., et al., *Understanding the roles of the P2X7 receptor in solid tumour progression and therapeutic perspectives.* Biochim Biophys Acta, 2015. **1848**(10 Pt B): p. 2584-602.
17. Pellegatti, P., et al., *A novel recombinant plasma membrane-targeted luciferase reveals a new pathway for ATP secretion.* Mol Biol Cell, 2005. **16**(8): p. 3659-65.
18. Pellegatti, P., et al., *Increased level of extracellular ATP at tumor sites: in vivo imaging with plasma membrane luciferase.* PLoS One, 2008. **3**(7): p. e2599.

19. Raffaghello, L., et al., *The P2X7 receptor sustains the growth of human neuroblastoma cells through a substance P-dependent mechanism.* Cancer Res, 2006. **66**(2): p. 907-14.
20. Wang, X., et al., *P2X7 receptor inhibition improves recovery after spinal cord injury.* Nat Med, 2004. **10**(8): p. 821-7.
21. Roger, S. and P. Pelegrin, *P2X7 receptor antagonism in the treatment of cancers.* Expert Opin Investig Drugs, 2011. **20**(7): p. 875-80.
22. Di Virgilio, F., *Purines, purinergic receptors, and cancer.* Cancer Res, 2012. **72**(21): p. 5441-7.
23. Apasov, S., et al., *Role of extracellular ATP and P1 and P2 classes of purinergic receptors in T-cell development and cytotoxic T lymphocyte effector functions.* Immunol Rev, 1995. **146**: p. 5-19.
24. Abbracchio, M.P., et al., *International Union of Pharmacology LVIII: update on the P2Y G protein-coupled nucleotide receptors: from molecular mechanisms and pathophysiology to therapy.* Pharmacol Rev, 2006. **58**(3): p. 281-341.
25. Newbolt, A., et al., *Membrane topology of an ATP-gated ion channel (P2X receptor).* J Biol Chem, 1998. **273**(24): p. 15177-82.
26. Kawate, T., et al., *Crystal structure of the ATP-gated P2X(4) ion channel in the closed state.* Nature, 2009. **460**(7255): p. 592-8.
27. Hattori, M. and E. Gouaux, *Molecular mechanism of ATP binding and ion channel activation in P2X receptors.* Nature, 2012. **485**(7397): p. 207-12.
28. North, R.A., *P2X receptors: a third major class of ligand-gated ion channels.* Ciba Found Symp, 1996. **198**: p. 91-105; discussion 105-9.
29. Surprenant, A., et al., *The cytolytic P2Z receptor for extracellular ATP identified as a P2X receptor (P2X7).* Science, 1996. **272**(5262): p. 735-8.
30. Jiang, L.H., et al., *Insights into the Molecular Mechanisms Underlying Mammalian P2X7 Receptor Functions and Contributions in Diseases, Revealed by Structural Modeling and Single Nucleotide Polymorphisms.* Front Pharmacol, 2013. **4**: p. 55.
31. Rassendren, F., et al., *The permeabilizing ATP receptor, P2X7. Cloning and expression of a human cDNA.* J Biol Chem, 1997. **272**(9): p. 5482-6.
32. Feng, Y.H., et al., *Endogenously expressed truncated P2X7 receptor lacking the C-terminus is preferentially upregulated in epithelial cancer cells and fails to mediate ligand-induced pore formation and apoptosis.* Nucleosides Nucleotides Nucleic Acids, 2006. **25**(9-11): p. 1271-6.
33. Cheewatrakoolpong, B., et al., *Identification and characterization of splice variants of the human P2X7 ATP channel.* Biochem Biophys Res Commun, 2005. **332**(1): p. 17-27.
34. Caseley, E.A., et al., *Non-synonymous single nucleotide polymorphisms in the P2X receptor genes: association with diseases, impact on receptor functions and potential use as diagnosis biomarkers.* Int J Mol Sci, 2014. **15**(8): p. 13344-71.
35. Bartlett, R., L. Stokes, and R. Sluyter, *The P2X7 receptor channel: recent developments and the use of P2X7 antagonists in models of disease.* Pharmacol Rev, 2014. **66**(3): p. 638-75.
36. Ferrari, D., et al., *The P2X7 receptor: a key player in IL-1 processing and release.* J Immunol, 2006. **176**(7): p. 3877-83.
37. Jiang, L.H., et al., *Subunit arrangement in P2X receptors.* J Neurosci, 2003. **23**(26): p. 8903-10.
38. Browne, L.E., L.H. Jiang, and R.A. North, *New structure enlivens interest in P2X receptors.* Trends Pharmacol Sci, 2010. **31**(5): p. 229-37.
39. Costa-Junior, H.M., F. Sarmento Vieira, and R. Coutinho-Silva, *C terminus of the P2X7 receptor: treasure hunting.* Purinergic Signal, 2011. **7**(1): p. 7-19.

40. North, R.A., *Molecular physiology of P2X receptors.* Physiol Rev, 2002. **82**(4): p. 1013-67.
41. Bradley, H.J., et al., *Pharmacological properties of the rhesus macaque monkey P2X7 receptor.* Br J Pharmacol, 2011. **164**(2b): p. 743-54.
42. Adinolfi, E., et al., *Expression of the P2X7 receptor increases the Ca2+ content of the endoplasmic reticulum, activates NFATc1, and protects from apoptosis.* J Biol Chem, 2009. **284**(15): p. 10120-8.
43. Browne, L.E., et al., *P2X7 receptor channels allow direct permeation of nanometer-sized dyes.* J Neurosci, 2013. **33**(8): p. 3557-66.
44. Roger, S., et al., *C-terminal calmodulin-binding motif differentially controls human and rat P2X7 receptor current facilitation.* J Biol Chem, 2010. **285**(23): p. 17514-24.
45. Roger, S., P. Pelegrin, and A. Surprenant, *Facilitation of P2X7 receptor currents and membrane blebbing via constitutive and dynamic calmodulin binding.* J Neurosci, 2008. **28**(25): p. 6393-401.
46. Sorge, R.E., et al., *Genetically determined P2X7 receptor pore formation regulates variability in chronic pain sensitivity.* Nat Med, 2012. **18**(4): p. 595-9.
47. Bianco, F., et al., *A role for P2X7 in microglial proliferation.* J Neurochem, 2006. **99**(3): p. 745-58.
48. Adinolfi, E., et al., *Trophic activity of a naturally occurring truncated isoform of the P2X7 receptor.* FASEB J, 2010. **24**(9): p. 3393-404.
49. Compan, V., et al., *P2X2 and P2X5 subunits define a new heteromeric receptor with P2X7-like properties.* J Neurosci, 2012. **32**(12): p. 4284-96.
50. Khakh, B.S., et al., *Neuronal P2X transmitter-gated cation channels change their ion selectivity in seconds.* Nat Neurosci, 1999. **2**(4): p. 322-30.
51. Virginio, C., et al., *Kinetics of cell lysis, dye uptake and permeability changes in cells expressing the rat P2X7 receptor.* J Physiol, 1999. **519 Pt 2**: p. 335-46.
52. Evans, R.J., et al., *Pharmacological characterization of heterologously expressed ATP-gated cation channels (P2x purinoceptors).* Mol Pharmacol, 1995. **48**(2): p. 178-83.
53. Adinolfi, E., et al., *Tyrosine phosphorylation of HSP90 within the P2X7 receptor complex negatively regulates P2X7 receptors.* J Biol Chem, 2003. **278**(39): p. 37344-51.
54. Ferrari, D., et al., *The antibiotic polymyxin B modulates P2X7 receptor function.* J Immunol, 2004. **173**(7): p. 4652-60.
55. Beigi, R.D., et al., *Oxidized ATP (oATP) attenuates proinflammatory signaling via P2 receptor-independent mechanisms.* Br J Pharmacol, 2003. **140**(3): p. 507-19.
56. Di Virgilio, F., et al., *Leukocyte P2 receptors: a novel target for anti-inflammatory and anti-tumor therapy.* Curr Drug Targets Cardiovasc Haematol Disord, 2005. **5**(1): p. 85-99.
57. Murgia, M., et al., *Oxidized ATP. An irreversible inhibitor of the macrophage purinergic P2Z receptor.* J Biol Chem, 1993. **268**(11): p. 8199-203.
58. Gargett, C.E. and J.S. Wiley, *The isoquinoline derivative KN-62 a potent antagonist of the P2Z-receptor of human lymphocytes.* Br J Pharmacol, 1997. **120**(8): p. 1483-90.
59. Baraldi, P.G., et al., *Synthesis and biological activity of N-arylpiperazine-modified analogues of KN-62, a potent antagonist of the purinergic P2X7 receptor.* J Med Chem, 2003. **46**(8): p. 1318-29.
60. Donnelly-Roberts, D.L. and M.F. Jarvis, *Discovery of P2X7 receptor-selective antagonists offers new insights into P2X7 receptor function and indicates a role in chronic pain states.* Br J Pharmacol, 2007. **151**(5): p. 571-9.

61. McGaraughty, S., et al., *P2X7-related modulation of pathological nociception in rats.* Neuroscience, 2007. **146**(4): p. 1817-28.
62. Donnelly-Roberts, D.L., et al., *Mammalian P2X7 receptor pharmacology: comparison of recombinant mouse, rat and human P2X7 receptors.* Br J Pharmacol, 2009. **157**(7): p. 1203-14.
63. Honore, P., et al., *A-740003 [N-(1-{[(cyanoimino)(5-quinolinylamino) methyl]amino}-2,2-dimethylpropyl)-2-(3,4-dimethoxyphenyl)acetamide], a novel and selective P2X7 receptor antagonist, dose-dependently reduces neuropathic pain in the rat.* J Pharmacol Exp Ther, 2006. **319**(3): p. 1376-85.
64. Michel, A.D., et al., *Direct labelling of the human P2X7 receptor and identification of positive and negative cooperativity of binding.* Br J Pharmacol, 2007. **151**(1): p. 103-14.
65. Michel, A.D., L.J. Chambers, and D.S. Walter, *Negative and positive allosteric modulators of the P2X(7) receptor.* Br J Pharmacol, 2008. **153**(4): p. 737-50.
66. Alcaraz, L., et al., *Novel P2X7 receptor antagonists.* Bioorg Med Chem Lett, 2003. **13**(22): p. 4043-6.
67. Burnstock, G. and G.E. Knight, *Cellular distribution and functions of P2 receptor subtypes in different systems.* Int Rev Cytol, 2004. **240**: p. 31-304.
68. Sperlagh, B., et al., *P2X7 receptors in the nervous system.* Prog Neurobiol, 2006. **78**(6): p. 327-46.
69. Lenertz, L.Y., et al., *Transcriptional control mechanisms associated with the nucleotide receptor P2X7, a critical regulator of immunologic, osteogenic, and neurologic functions.* Immunol Res, 2011. **50**(1): p. 22-38.
70. Wiley, J.S., et al., *The human P2X7 receptor and its role in innate immunity.* Tissue Antigens, 2011. **78**(5): p. 321-32.
71. Di Virgilio, F., *Liaisons dangereuses: P2X(7) and the inflammasome.* Trends Pharmacol Sci, 2007. **28**(9): p. 465-72.
72. Ferrari, D., et al., *Extracellular ATP triggers IL-1 beta release by activating the purinergic P2Z receptor of human macrophages.* J Immunol, 1997. **159**(3): p. 1451-8.
73. Hewinson, J. and A.B. Mackenzie, *P2X(7) receptor-mediated reactive oxygen and nitrogen species formation: from receptor to generators.* Biochem Soc Trans, 2007. **35**(Pt 5): p. 1168-70.
74. Miller, C.M., et al., *The role of the P2X(7) receptor in infectious diseases.* PLoS Pathog, 2011. **7**(11): p. e1002212.
75. Di Virgilio, F., *The therapeutic potential of modifying inflammasomes and NOD-like receptors.* Pharmacol Rev, 2013. **65**(3): p. 872-905.
76. Qu, Y. and G.R. Dubyak, *P2X7 receptors regulate multiple types of membrane trafficking responses and non-classical secretion pathways.* Purinergic Signal, 2009. **5**(2): p. 163-73.
77. Pupovac, A., L. Stokes, and R. Sluyter, *CAY10593 inhibits the human P2X7 receptor independently of phospholipase D1 stimulation.* Purinergic Signal, 2013. **9**(4): p. 609-19.
78. Di Virgilio, F., et al., *Extracellular ATP as a possible mediator of cell-mediated cytotoxicity.* Immunol Today, 1990. **11**(8): p. 274-7.
79. Zanovello, P., et al., *Responses of mouse lymphocytes to extracellular ATP. II. Extracellular ATP causes cell type-dependent lysis and DNA fragmentation.* J Immunol, 1990. **145**(5): p. 1545-50.
80. Chow, S.C., G.E. Kass, and S. Orrenius, *Purines and their roles in apoptosis.* Neuropharmacology, 1997. **36**(9): p. 1149-56.

81. Weiss, B., *Differential activation and inhibition of the multiple forms of cyclic nucleotide phosphodiesterase.* Adv Cyclic Nucleotide Res, 1975. **5**: p. 195-211.
82. Yip, L., et al., *Autocrine regulation of T-cell activation by ATP release and P2X7 receptors.* FASEB J, 2009. **23**(6): p. 1685-93.
83. Adinolfi, E., et al., *Basal activation of the P2X7 ATP receptor elevates mitochondrial calcium and potential, increases cellular ATP levels, and promotes serum-independent growth.* Mol Biol Cell, 2005. **16**(7): p. 3260-72.
84. Monif, M., et al., *The P2X7 receptor drives microglial activation and proliferation: a trophic role for P2X7R pore.* J Neurosci, 2009. **29**(12): p. 3781-91.
85. Amoroso, F., et al., *The P2X7 receptor is a key modulator of aerobic glycolysis.* Cell Death Dis, 2012. **3**: p. e370.
86. Slater, M., et al., *Differentiation between cancerous and normal hyperplastic lobules in breast lesions.* Breast Cancer Res Treat, 2004. **83**(1): p. 1-10.
87. Slater, M., et al., *Early prostate cancer detected using expression of non-functional cytolytic P2X7 receptors.* Histopathology, 2004. **44**(3): p. 206-15.
88. Adinolfi, E., et al., *Expression of P2X7 receptor increases in vivo tumor growth.* Cancer Res, 2012. **72**(12): p. 2957-69.
89. Li, X., et al., *The P2X7 receptor: a novel biomarker of uterine epithelial cancers.* Cancer Epidemiol Biomarkers Prev, 2006. **15**(10): p. 1906-13.
90. Amoroso, F., et al., *The P2X7 receptor is a key modulator of the PI3K/GSK3beta/VEGF signaling network: evidence in experimental neuroblastoma.* Oncogene, 2015. **34**(41): p. 5240-51.
91. White, N., P.E. Butler, and G. Burnstock, *Human melanomas express functional P2 X(7) receptors.* Cell Tissue Res, 2005. **321**(3): p. 411-8.
92. Solini, A., et al., *Increased P2X7 receptor expression and function in thyroid papillary cancer: a new potential marker of the disease?* Endocrinology, 2008. **149**(1): p. 389-96.
93. Ghalali, A., et al., *Atorvastatin prevents ATP-driven invasiveness via P2X7 and EHBP1 signaling in PTEN-expressing prostate cancer cells.* Carcinogenesis, 2014. **35**(7): p. 1547-55.
94. Li, X., et al., *Decreased expression of P2X7 in endometrial epithelial pre-cancerous and cancer cells.* Gynecol Oncol, 2007. **106**(1): p. 233-43.
95. Feng, Y.H., et al., *A truncated P2X7 receptor variant (P2X7-j) endogenously expressed in cervical cancer cells antagonizes the full-length P2X7 receptor through hetero-oligomerization.* J Biol Chem, 2006. **281**(25): p. 17228-37.
96. Adinolfi, E., et al., *P2X7 receptor expression in evolutive and indolent forms of chronic B lymphocytic leukemia.* Blood, 2002. **99**(2): p. 706-8.
97. Chong, J.H., et al., *Abnormal expression of P2X family receptors in Chinese pediatric acute leukemias.* Biochem Biophys Res Commun, 2010. **391**(1): p. 498-504.
98. Chong, J.H., et al., *The hyposensitive N187D P2X7 mutant promotes malignant progression in nude mice.* J Biol Chem, 2010. **285**(46): p. 36179-87.
99. Jelassi, B., et al., *P2X(7) receptor activation enhances SK3 channels- and cystein cathepsin-dependent cancer cells invasiveness.* Oncogene, 2011. **30**(18): p. 2108-22.
100. Clark, A.K., et al., *Cathepsin S release from primary cultured microglia is regulated by the P2X7 receptor.* Glia, 2010. **58**(14): p. 1710-26.
101. Gu, B.J. and J.S. Wiley, *Rapid ATP-induced release of matrix metalloproteinase 9 is mediated by the P2X7 receptor.* Blood, 2006. **107**(12): p. 4946-53.

102. Takai, E., et al., *Autocrine regulation of TGF-beta1-induced cell migration by exocytosis of ATP and activation of P2 receptors in human lung cancer cells.* J Cell Sci, 2012. **125**(Pt 21): p. 5051-60.
103. Jelassi, B., et al., *Anthraquinone emodin inhibits human cancer cell invasiveness by antagonizing P2X7 receptors.* Carcinogenesis, 2013. **34**(7): p. 1487-96.
104. Giannuzzo, A., S.F. Pedersen, and I. Novak, *The P2X7 receptor regulates cell survival, migration and invasion of pancreatic ductal adenocarcinoma cells.* Mol Cancer, 2015. **14**(1): p. 203.
105. Hanahan, D. and R.A. Weinberg, *Hallmarks of cancer: the next generation.* Cell, 2011. **144**(5): p. 646-74.
106. de Visser, K.E. and L.M. Coussens, *The inflammatory tumor microenvironment and its impact on cancer development.* Contrib Microbiol, 2006. **13**: p. 118-37.
107. Fernando, K.C., C.E. Gargett, and J.S. Wiley, *Activation of the P2Z/P2X7 receptor in human lymphocytes produces a delayed permeability lesion: involvement of phospholipase D.* Arch Biochem Biophys, 1999. **362**(2): p. 197-202.
108. Gudipaty, L., et al., *Essential role for Ca2+ in regulation of IL-1beta secretion by P2X7 nucleotide receptor in monocytes, macrophages, and HEK-293 cells.* Am J Physiol Cell Physiol, 2003. **285**(2): p. C286-99.
109. Mutini, C., et al., *Mouse dendritic cells express the P2X7 purinergic receptor: characterization and possible participation in antigen presentation.* J Immunol, 1999. **163**(4): p. 1958-65.
110. Aymeric, L., et al., *Tumor cell death and ATP release prime dendritic cells and efficient anticancer immunity.* Cancer Res, 2010. **70**(3): p. 855-8.
111. Martins, I., et al., *Chemotherapy induces ATP release from tumor cells.* Cell Cycle, 2009. **8**(22): p. 3723-8.
112. Martinon, F. and J. Tschopp, *Inflammatory caspases and inflammasomes: master switches of inflammation.* Cell Death Differ, 2007. **14**(1): p. 10-22.
113. Eisenbarth, S.C., et al., *Crucial role for the Nalp3 inflammasome in the immunostimulatory properties of aluminium adjuvants.* Nature, 2008. **453**(7198): p. 1122-6.
114. Ghiringhelli, F., et al., *Activation of the NLRP3 inflammasome in dendritic cells induces IL-1beta-dependent adaptive immunity against tumors.* Nat Med, 2009. **15**(10): p. 1170-8.
115. Wilhelm, K., et al., *Graft-versus-host disease is enhanced by extracellular ATP activating P2X7R.* Nat Med, 2010. **16**(12): p. 1434-8.
116. Vergani, A., et al., *Long-term heart transplant survival by targeting the ionotropic purinergic receptor P2X7.* Circulation, 2013. **127**(4): p. 463-75.
117. Vergani, A., et al., *Effect of the purinergic inhibitor oxidized ATP in a model of islet allograft rejection.* Diabetes, 2013. **62**(5): p. 1665-75.
118. Adinolfi, E., et al., *Accelerated tumor progression in mice lacking the ATP receptor P2X7.* Cancer Res, 2015. **75**(4): p. 635-44.
119. Diaz-Hernandez, M., et al., *Inhibition of the ATP-gated P2X7 receptor promotes axonal growth and branching in cultured hippocampal neurons.* J Cell Sci, 2008. **121**(Pt 22): p. 3717-28.
120. Airoldi, I., et al., *Endogenous IL-12 triggers an antiangiogenic program in melanoma cells.* Proc Natl Acad Sci U S A, 2007. **104**(10): p. 3996-4001.
121. Michaud, M., et al., *Autophagy-dependent anticancer immune responses induced by chemotherapeutic agents in mice.* Science, 2011. **334**(6062): p. 1573-7.
122. Syberg, S., et al., *Genetic Background Strongly Influences the Bone Phenotype of P2X7 Receptor Knockout Mice.* J Osteoporos, 2012. **2012**: p. 391097.

123. Sjoo, F., et al., *Myeloablative and immunosuppressive properties of treosulfan in mice.* Exp Hematol, 2006. **34**(1): p. 115-21.
124. Sangaletti, S., et al., *Leukocyte, rather than tumor-produced SPARC, determines stroma and collagen type IV deposition in mammary carcinoma.* J Exp Med, 2003. **198**(10): p. 1475-85.
125. Inaba, K., et al., *Generation of large numbers of dendritic cells from mouse bone marrow cultures supplemented with granulocyte/macrophage colony-stimulating factor.* J Exp Med, 1992. **176**(6): p. 1693-702.
126. Giuliani, A.L., et al., *Changes in murine bone marrow macrophages and erythroid burst-forming cells following the intravenous injection of liposome-encapsulated dichloromethylene diphosphonate (Cl2MDP).* Eur J Haematol, 2001. **66**(4): p. 221-9.
127. Adriouch, S., et al., *Cutting edge: a natural P451L mutation in the cytoplasmic domain impairs the function of the mouse P2X7 receptor.* J Immunol, 2002. **169**(8): p. 4108-12.
128. Dinarello, C.A., *A clinical perspective of IL-1beta as the gatekeeper of inflammation.* Eur J Immunol, 2011. **41**(5): p. 1203-17.
129. Dunn, J.H., L.Z. Ellis, and M. Fujita, *Inflammasomes as molecular mediators of inflammation and cancer: potential role in melanoma.* Cancer Lett, 2012. **314**(1): p. 24-33.
130. Ferrari, D., et al., *Mouse microglial cells express a plasma membrane pore gated by extracellular ATP.* J Immunol, 1996. **156**(4): p. 1531-9.
131. Labasi, J.M., et al., *Absence of the P2X7 receptor alters leukocyte function and attenuates an inflammatory response.* J Immunol, 2002. **168**(12): p. 6436-45.
132. Barbera-Cremades, M., et al., *P2X7 receptor-stimulation causes fever via PGE2 and IL-1beta release.* FASEB J, 2012. **26**(7): p. 2951-62.
133. Asgari, E., et al., *C3a modulates IL-1beta secretion in human monocytes by regulating ATP efflux and subsequent NLRP3 inflammasome activation.* Blood, 2013. **122**(20): p. 3473-81.
134. Quail, D.F. and J.A. Joyce, *Microenvironmental regulation of tumor progression and metastasis.* Nat Med, 2013. **19**(11): p. 1423-37.
135. Antonioli, L., et al., *Immunity, inflammation and cancer: a leading role for adenosine.* Nat Rev Cancer, 2013. **13**(12): p. 842-57.
136. Becker, M.A., et al., *Dual HER/VEGF receptor targeting inhibits in vivo ovarian cancer tumor growth.* Mol Cancer Ther, 2013. **12**(12): p. 2909-16.
137. Burnstock, G., *Purinergic signalling--an overview.* Novartis Found Symp, 2006. **276**: p. 26-48; discussion 48-57, 275-81.
138. Forrester, T., *An estimate of adenosine triphosphate release into the venous effluent from exercising human forearm muscle.* J Physiol, 1972. **224**(3): p. 611-28.
139. Falzoni, S., G. Donvito, and F. Di Virgilio, *Detecting adenosine triphosphate in the pericellular space.* Interface Focus, 2013. **3**(3): p. 20120101.
140. Coutinho-Silva, R., et al., *The P2X(7) receptor and intracellular pathogens: a continuing struggle.* Purinergic Signal, 2009. **5**(2): p. 197-204.
141. Bours, M.J., et al., *P2 receptors and extracellular ATP: a novel homeostatic pathway in inflammation.* Front Biosci (Schol Ed), 2011. **3**: p. 1443-56.
142. Di Virgilio, F., *Dr. Jekyll/Mr. Hyde: the dual role of extracellular ATP.* J Auton Nerv Syst, 2000. **81**(1-3): p. 59-63.
143. Rayah, A., J.M. Kanellopoulos, and F. Di Virgilio, *P2 receptors and immunity.* Microbes Infect, 2012. **14**(14): p. 1254-62.
144. Burnstock, G. and F. Di Virgilio, *Purinergic signalling and cancer.* Purinergic Signal, 2013. **9**(4): p. 491-540.

145. Hill, L.M., et al., *Extracellular ATP may contribute to tissue repair by rapidly stimulating purinergic receptor X7-dependent vascular endothelial growth factor release from primary human monocytes.* J Immunol, 2010. **185**(5): p. 3028-34.
146. Junger, W.G., *Immune cell regulation by autocrine purinergic signalling.* Nat Rev Immunol, 2011. **11**(3): p. 201-12.
147. Falzoni, S., et al., *The purinergic P2Z receptor of human macrophage cells. Characterization and possible physiological role.* J Clin Invest, 1995. **95**(3): p. 1207-16.
148. da Silva, G.L., et al., *P2X7 receptor is required for neutrophil accumulation in a mouse model of irritant contact dermatitis.* Exp Dermatol, 2013. **22**(3): p. 184-8.
149. Goel, H.L. and A.M. Mercurio, *VEGF targets the tumour cell.* Nat Rev Cancer, 2013. **13**(12): p. 871-82.